

Excitation of magnetospheric waveguide modes by magnetosheath flows

Ian R. Mann¹

Department of Physics, University of Alberta, Edmonton, Alberta, Canada

Andrew N. Wright, Katharine J. Mills, and Valery M. Nakariakov

Mathematical Institute, University of St. Andrews, St. Andrews, Fife, Scotland

Abstract. Standard models of the Earth's outer magnetospheric waveguide assume that a perfectly reflecting magnetopause can trap energy inside the waveguide. In contrast, we show that the near-noon magnetopause often acts as a leaky boundary, wave trapping only being possible for large magnetosheath flow speeds. Moreover, for sufficiently fast flow speeds, we show how waveguide modes may be energized by magnetosheath flows via the overreflection mechanism. Unbounded simulations of the growth of surface waves via the development of a Kelvin-Helmholtz instability (KHI) vortex sheet show growth rates which increase without limit proportional to wavenumber (k_y), until the assumption of a thin boundary is no longer valid. For a bounded magnetosphere, however, overreflected body type waveguide modes can introduce wavenumber selection, that is, generate modes with maximum linear growth rates at finite k_y . A necessary condition is that the wave is propagating in the magnetosphere, that is, the wave's turning point lies inside the magnetosphere. By developing a new description of both KHI and waveguide mode growth in terms of overreflection and the propagation of negative energy waves, we show how the maximum growth rate can be understood in terms of the reflection coefficient of waves incident upon the magnetopause. Our model can also explain the observed local time dependence of $Pc5$ field line resonance wave power, and can explain the observed correlation between high solar wind speeds and $Pc5$ wave power. Finally, we show how a waveguide with a free magnetopause boundary supports quarter-wavelength modes. These modes have lower frequencies than the standard (magnetopause velocity node) half-wavelength modes, perhaps generating the millihertz waveguide mode eigenfrequencies which appear to drive field line resonances in HF radar data.

1. Introduction

The possibility that the magnetopause can be subject to the Kelvin-Helmholtz instability (KHI) had been known for over 4 decades [e.g., Dungey, 1955; Parker, 1958]. The compressional KHI can generate unstable (growing) surface waves on the magnetopause, and these have been suggested as energy sources for low azimuthal wavenumber (m) $Pc5$ ULF pulsations through the field line resonance (FLR) mechanism [Southwood, 1974; Chen and Hasegawa, 1974a,b]. Later modifications to the FLR theory suggested waves could be driven

by radially standing compressional disturbances, rather than surface waves, and resulted in magnetospheric cavity mode theory [Kivelson et al., 1984; Kivelson and Southwood, 1985, 1986]. Unlike surface modes, the cavity modes do not have amplitudes which decay exponentially away from the magnetopause, and they can hence more easily drive FLRs deep in the magnetosphere. Moreover, the frequency spectrum of the cavity modes is structured by the magnetospheric cavity ringing at its natural frequencies. The cavity model has since been refined with the introduction of the waveguide model, whereby the cavity remains open downtail [Samson et al., 1992; Harrold and Samson, 1992; Wright, 1994; Rickard and Wright, 1994]. In this case, waveguide modes propagate antisunward down the waveguide but still have frequencies which are determined by the natural frequencies of the magnetosphere. It is possible that waveguide modes can be driven by either solar wind impulses near the magnetospheric nose (see,

¹Now at Department of Physics, University of York, Heslington, York, England.

for example, the recent observations of *Mann et al.* [1998]), or by magnetopause instabilities on the flanks [e.g., *Ziesolleck and McDiarmid*, 1994], depending upon solar wind conditions.

Interestingly, a consideration of the theoretical excitation of waveguide modes has received little attention to date. In a series of papers, Allan and his coworkers considered the excitation of cavity modes by simplified driving terms [e.g., *Allan et al.*, 1985, 1986]. Similarly, *Southwood and Kivelson* [1990] considered the excitation of magnetospheric cavities by sudden impulses, while *Wright and Rickard* [1995a] considered random buffeting. However, almost all cavity or waveguide simulations consider the magnetopause to act as a perfectly reflecting rigid boundary. Consequently, the excitation of waveguide modes by magnetopause instabilities cannot be considered (since the magnetopause is fixed). In a very recent paper, A. D. M. Walker (Excitation of magnetohydrodynamic cavities in the magnetosphere, submitted to *Journal of Atmospheric, Solar, and Terrestrial Physics*, 1998) considered the trapping of magnetospheric cavity modes excited by the transmission of waves from the solar wind across the magnetopause. However, Walker set the magnetosheath flow speed to zero, so that neither the effect of flows on wave trapping nor the excitation of waves by magnetosheath flows was considered. In this paper we consider a waveguide model which is bounded by a free magnetopause, and investigate the energization of waveguide modes by magnetosheath flows.

Early work on the KHI considered the stability of the vortex sheet separating unbounded, incompressible plasma flows [e.g., *Chandrasekhar*, 1961]. Later work showed how the inclusion of plasma compressibility has an important effect on the KHI [e.g., *Sen*, 1964; *Fejer*, 1964; *Southwood*, 1968; *Ong and Roderick*, 1972; *Pu and Kivelson*, 1983]. In an incompressible plasma the phase velocity of a KH wave is aligned with the boundary between the two flowing plasmas. In contrast, the compressible KHI generates a component of wave phase velocity perpendicular to the boundary [*Pu and Kivelson*, 1983]. The direction of the phase velocity of waves driven by magnetopause instabilities, and the resulting energy transport, form important aspects of our analysis and are topics to which we return later in the paper.

Standard treatments of the unbounded compressible KHI (with the components of the wavenumber in the vortex sheet held fixed) have shown that the KHI has both upper and lower cutoff flow speeds, the waves being stable for flow speeds less/greater than the lower/upper cutoff speeds, respectively. The lower cutoff speed (U_c) is due to the stabilizing action of magnetic field tension; U_c for a mode propagating parallel to the flow is given by the Alfvén speed calculated using the component of the magnetic field parallel to the flow [e.g., *Miura*, 1992]. The existence of the upper cutoff speed (U_u) for unbounded compressible plasmas [e.g., *Fejer*, 1964; *Sen*, 1964; *Pu and Kivelson*, 1983]

corresponds physically to the situation where the phase speed of the wave reaches the fast magnetoacoustic speed in either of the bounding media. In that case the waves change from being spatially evanescent (surface type) modes to spatially oscillatory (body type) modes which propagate away from the boundary and stabilize the KHI. Since the waves can now transport energy away from the interface, the solution does not grow exponentially in time, as is the case for the surface waves which confine energy to the vicinity of the interface. Introducing an inner boundary, however, such as a turning point in the magnetosphere, can allow the propagating (body) waves to become trapped in a magnetospheric cavity. If the magnetopause continues to be unstable, then this can result in the modes becoming energized by magnetosheath flows, and introduces the possibility that magnetopause instabilities can generate unstable (growing) body modes, in addition to the more well known KHI-generated surface modes.

For a vortex sheet the growth rate of the instability increases without limit with increasing wavenumber parallel to the flow. Mathematically, the problem is ill-posed, and ultimately results in an inconsistency whereby the assumption that the wave's scale length remains much larger than the width of the boundary layer is no longer satisfied [e.g., *Lerche*, 1966]. Similarly, the MHD approximation breaks down once the scale lengths approach kinetic scale lengths such as the ion gyroradius. This led researchers to investigate the stability of unbounded media, separated by a shear flow boundary layer of finite thickness [e.g., *Ong and Roderick*, 1972]. The introduction of the feature of finite thickness stabilizes the high wavenumber modes, and generates a KH wave with a maximum growth rate at a finite wavenumber [e.g., *Walker*, 1981; *Miura and Pritchett*, 1982]. Moreover, the fact that the change in the velocity of the shear layer happens over a finite width removes the upper KH cutoff speed, and allows the waves to be unstable for any (even superfast magnetoacoustic) flow speed [*Papamoshou and Roshko*, 1988; *Miura*, 1992].

Interestingly, by introducing an inner boundary, it is also possible to stabilize the high azimuthal wavenumber modes. Until recently, the effect of introducing an inner magnetospheric boundary on magnetopause instabilities has received little attention. *Fujita et al.* [1996] considered the MHD eigenmodes supported by a bounded nonuniform magnetosphere, connected via an infinitesimal free magnetopause to a flowing magnetosheath, and concentrated on the behavior of KH surface waves. Their bounded model showed that under conditions of large magnetosheath flow speeds, waves could possess maximum growth rates at finite wavenumbers, and they attributed this spectral structuring to the assumed nonuniformity in the magnetosphere in their model.

In this paper we consider a similar model to *Fujita et al.* [1996]; however, we consider the behavior of both surface and body type solutions. To elucidate the im-

portant physics, we consider both the bounded magnetosphere and the unbounded magnetosheath to be uniform, and show that nonuniformity is not a necessity for wavenumber selection. Simply introducing a boundary in the magnetosphere can select a wavenumber with a maximum growth rate. We show that a necessary condition is that the waves' phase speed is superfast magnetoacoustic in the magnetosphere; that is, the turning point of the waves lies inside the magnetosphere, and hence the mode is of body type and has a spatially oscillatory character inside the magnetopause. This is reasonable, since if the natural frequencies of the magnetosphere are to determine the frequencies of the modes, as is postulated in waveguide mode theory, then the modes must be propagating between the magnetopause and their turning point.

We also present a new interpretation of the KHI, and for the energization of waveguide modes, by considering the reflection and transmission of waves incident upon the magnetopause. We employ the concepts of wave overreflection and negative energy waves [Landau and Lifshitz, 1987; also McKenzie, 1970] and show how this reveals an understanding of the physics of the interaction of the flowing magnetosheath with the stationary magnetosphere. The growth of the waves and the existence of the maximum growth rate at finite wavenumber can be understood in terms of this wave overreflection.

Standard waveguide treatments assume a perfectly reflecting magnetopause, and generate half-wavelength modes between the magnetopause and the turning point. In contrast, we show that for typical magnetospheric parameters the magnetopause often acts as a leaky boundary. Increasing the flow speed allows the boundary to become reflecting, with wave overreflection allowing an energization of the waveguide mode harmonics when the magnetosheath flow speed is sufficiently fast. This may explain both the localization of Pc5 wave power on the flanks and the observed correlation between large solar wind flow speeds and Pc5 wave power in the outer magnetosphere [e.g., Engebretson et al., 1998].

We also show how the waves driven in our model are often quarter-wavelength harmonics. The free magnetopause boundary allows the waves to approach a velocity antinode at the magnetopause, and generates quarter-wavelength modes. These new waveguide modes have lower frequencies than the usual (velocity) nodal waveguide mode harmonics, and this may provide an explanation for the low (millihertz) frequencies of FLRs which are believed to be driven by the waveguide modes. Consequently, our investigation of the excitation of the waveguide modes strengthens waveguide mode theory further by providing an explanation for the excitation of waveguide modes with preferred azimuthal wavenumbers (m is a free parameter in standard cavity mode treatments), and offers a possible mechanism for generating low-frequency (millihertz) waveguide modes by proposing a consideration of quarter-wavelength modes.

The paper is structured as follows: Section 2 presents our model and the governing equations; section 3 introduces the concepts of wave reflection and overreflection; section 4 presents the results from our simulations; and section 5 discusses them in the context of magnetospheric pulsations. Finally, section 6 summarizes our paper.

2. Model

In this paper we consider a simplified compressible MHD model consisting of a bounded magnetosphere, separated by a sheet magnetopause from a semi-infinite flowing magnetosheath. For simplicity, both the magnetosphere and the magnetosheath are assumed to be uniform. The magnetosphere is cold, has a uniform density ρ_0 , and is permeated by a uniform magnetic field $\mathbf{B}_0 = B_0 \hat{\mathbf{z}}$. The magnetosheath is assumed to be field free, has a plasma density ρ_e and a background plasma pressure P_e , and is flowing parallel to the magnetopause boundary (which lies in the y - z plane) with a velocity $\mathbf{U} = U \hat{\mathbf{y}}$. The inner boundary of the magnetosphere is perfectly reflecting and lies at $x = d$, while the magnetopause lies at $x = 0$ (the $\hat{\mathbf{x}}$ direction pointing from the magnetopause into the magnetosphere). The model geometry is illustrated in Figure 1. An important parameter in the simulations is $\delta = c_s/c_A$, where $c_s^2 = \gamma P_e/\rho_e$, $c_A^2 = B_0^2/\mu_0 \rho_0$, and γ is the ratio of specific heats, taken to be 5/3. Once we choose δ , the background density ratio ρ_0/ρ_e is given from zeroth order pressure balance as $\rho_0/\rho_e = 6\delta^2/5$.

In the magnetosphere we consider linear waves which vary $\sim \exp i(\omega t - k_z z - k_y y - k_x x)$, and in the magnetosheath $\sim \exp i(\omega t - k_z z - k_y y - \kappa x)$. The wavenumbers k_x and κ are given by the dispersion relations for fast magnetoacoustic modes

$$k_z^2 = \frac{\omega^2}{c_A^2} - k_y^2 - k_x^2 \quad (1)$$

$$\kappa^2 = \frac{(\omega - U k_y)^2}{c_s^2} - k_y^2 - k_z^2. \quad (2)$$

In a nonuniform magnetosphere, Alfvén waves can be excited at locations where the eigenfrequencies of the fast waves match the local Alfvén eigenfrequencies. Our model considers uniform plasmas, so that the fast and Alfvén waves are decoupled. Moreover, we choose $k_z = 0$ to remove the Alfvén mode from the simulations. This allows us to examine the excitation of fast magnetospheric waveguide modes by magnetosheath flows without the complication of the waves coupling energy into a field line resonance and yields considerable insight on the excitation of the fast waveguide modes.

MHD wave solutions on either side of the magnetopause are connected through two boundary conditions at $x = 0$. First, the total pressure is assumed to be continuous (lest the boundary suffer infinite acceleration), and second the normal linear displacement on each side

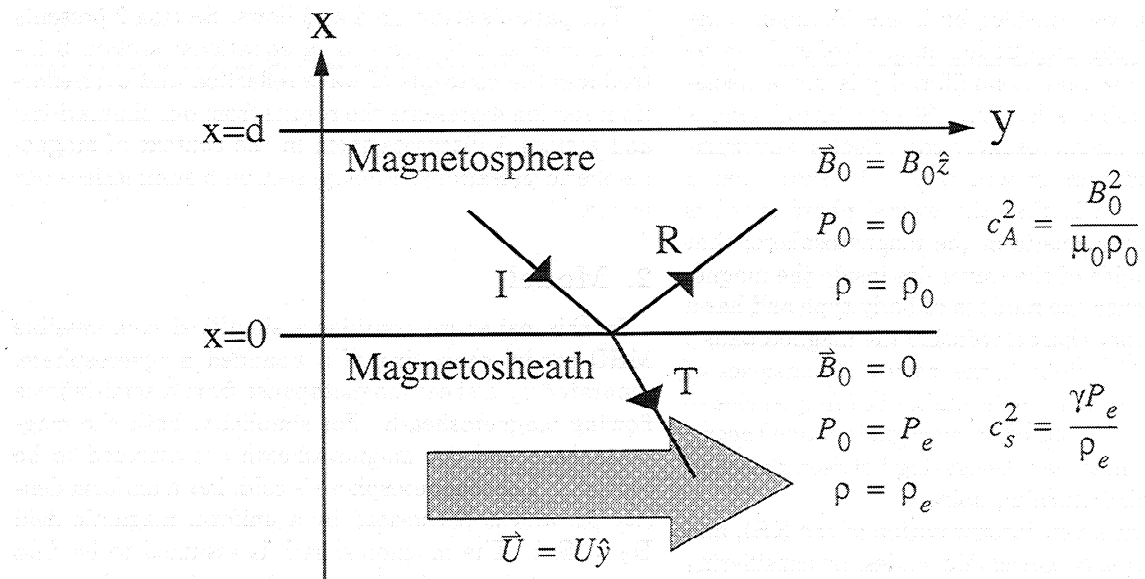


Figure 1. Schematic diagram of the model magnetosphere and magnetosheath. Also shown are schematic incident (I), reflected (R), and transmitted (T) rays of waves incident upon the magnetopause.

of the undisturbed boundary must be continuous (so that there is no cavitation). Considering the normal magnetopause displacement ξ to have the same form as the waves driving the motion (which follows from linearity), that is, $\xi(y, t) = \xi_0 \exp i(\omega t - k_y y)$, the normal velocity of the disturbed boundary v_x is given by [e.g., Lamb, 1932]

$$v_x = \frac{D\xi}{Dt}. \quad (3)$$

Equating ξ from the velocities v_{x0} and v_{xe} on each side of the interface results in the boundary condition

$$\frac{v_{xe}}{(\omega - U k_y)} = \frac{v_{x0}}{\omega}. \quad (4)$$

Note that although the normal displacement must be continuous, it is the quantity $v_x/(\omega - U k_y)$ which must be continuous across the boundary and not v_x (cf. equation (18), page 482, of Chandrasekhar [1961]). The perturbation v_x will only vary continuously if the background velocity U also varies continuously. The inner magnetospheric boundary is assumed to be perfectly reflecting, so that $v_x|_{x=d} = 0$, from which it also follows that $dP_T/dx|_{x=d} = 0$, where P_T is the total pressure perturbation.

With these boundary conditions, fast MHD wave modes are governed by the equation

$$\tan k_x d + i \frac{\rho_0}{\rho_e} \frac{\kappa}{k_x} \frac{\omega^2}{(\omega - U k_y)^2} = 0 \quad (5)$$

with k_x and κ given by (1) and (2) above. Here, $\omega = \omega_r + i\omega_i$, $k_x = k_{xr} + ik_{xi}$ and $\kappa = \kappa_r + i\kappa_i$. Consequently, (5) can describe waves which are either spatially oscillatory, or evanescent, or both, in each of the

magnetosphere and magnetosheath, and can be stable ($\omega_i = 0$), or growing or decaying ($\omega_i < 0$ or > 0 respectively).

Equation (5) is a transcendental equation which we solve numerically using a Newton-Raphson scheme for the complex eigenvalues $\omega = \omega_r + i\omega_i$. The dispersion relations (1) and (2) contain solutions which can be propagating in either the positive or negative \hat{x} directions. In the magnetosphere the solutions are independent of the sign of the square root for k_x in (1); however, in the magnetosheath, choosing the sign of κ in (2) selects waves whose phase propagates toward or away from the magnetosphere. We choose $\omega_r > 0$, and select κ_r to ensure that the phase of the waves in the flowing magnetosheath frame propagates away from the magnetosphere toward $x \rightarrow -\infty$. With the real part of the Doppler-shifted flow frame frequency $\omega'_r = \omega_r - U k_y$, then since the waves in the magnetosheath flow frame vary $\sim \exp i(\omega' t - \kappa x)$, we have $\kappa_r < 0$ when $\omega'_r > 0$, and $\kappa_r > 0$ when $\omega'_r < 0$. If $\kappa_r = 0$, we choose the solution which decays exponentially as $x \rightarrow -\infty$ (i.e., $\kappa_i > 0$).

3. Wave Reflection and Overreflection

Central to the theme of this paper is the question of how energy is transported from the flowing magnetosheath, across the magnetopause, and into the magnetosphere. Physical understanding of this problem can be gained from a consideration of the reflection of waves incident upon the magnetopause from the magnetosphere (see the schematic rays shown in Figure 1). Considering an incident wave of unit amplitude ($I = 1$), being reflected with a reflection coefficient R , and trans-

mitted into the magnetosheath with a transmission coefficient T , then the total pressure perturbation in the magnetosphere

$$p_{T0} = \exp i(\omega t - k_y y) \{ \exp ik_x x + R \exp -ik_x x \}, \quad (6)$$

and in the magnetosheath

$$p_{Te} = T \exp i(\omega t - k_y y) \exp -ikx. \quad (7)$$

The linear boundary conditions on the continuity of total pressure, and normal displacement on the magnetopause result in the conditions

$$1 + R = T \quad (8)$$

$$\frac{\kappa T}{\rho_e} \frac{1}{(\omega - U k_y)^2} = \frac{k_x (R - 1)}{\rho_0 \omega^2} \quad (9)$$

which can be solved to give

$$R = \frac{k_x \rho_e (\omega - U k_y)^2 + \kappa \rho_0 \omega^2}{k_x \rho_e (\omega - U k_y)^2 - \kappa \rho_0 \omega^2}. \quad (10)$$

As discussed in section 2, we choose the sign of κ_r to give waves which propagate away from the magnetopause in the magnetosheath flow frame.

Waves incident upon the magnetopause from the magnetosphere can be (1) perfectly reflected ($|R| = 1$), (2) partially transmitted ($|R| < 1$), or (3) overreflected ($|R| > 1$). In case 1, the magnetosheath wave solution is exponentially decaying toward $x = -\infty$, so $\kappa_r = 0$, and $\kappa_i > 0$. With a bounded magnetosphere, modal solutions to (5) which experience perfect magnetopause reflection represent trapped body modes which have $\omega_r \neq 0$ and $\omega_i = 0$ [Roberts, 1991], and are the free magnetopause boundary representations of the rigid boundary trapped cavity/waveguide modes.

In cases 2 and 3, $\kappa_r \neq 0$ and the magnetosheath solutions contain phase which propagates in either the $\pm \hat{x}$ direction. Whether the waves grow or decay depends upon a consideration of the direction of propagation of the waves' phase and group velocities. The \hat{x} component of the group velocity of the waves is given by

$$v_g = \frac{\partial \omega}{\partial \kappa} = \frac{c_s^2 \kappa}{\omega'}, \quad (11)$$

the real part being equal to

$$\text{Re}(v_g) = \frac{c_s^2 (\kappa_r \omega'_r + \kappa_i \omega'_i)}{|\omega'|^2}. \quad (12)$$

Since a single mode will satisfy the magnetosheath dispersion relation, then taking the imaginary parts of the dispersion relation we have $\omega'_r / \kappa_r = c_s^2 \kappa_i / \omega'_i$. As the choice of the positive or negative root for κ_r changes when ω'_r changes sign ($\omega'_r \gtrless 0$ when $\kappa_r \lesseqgtr 0$, as described at the end of section 2), then it follows that the sign of the two terms in the parentheses in (12) will always be the same and be negative. Hence the (real) group ve-

locity is always directed away from the magnetosphere toward $x = -\infty$. Interestingly, while wave momentum is a frame independent quantity, energy density is frame dependent. *McKenzie* [1970] provided an elegant discussion of this, and shows that wave energy density is given by

$$\epsilon = \epsilon_0 \frac{\omega}{\omega'}. \quad (13)$$

Here ϵ_0 is the wave energy density in the fluid rest frame (as defined, for example, by *Anderson* [1963]). *McKenzie* [1970] showed that waves with negative energy in the rest frame of a flowing medium have opposite directions of phase propagation in the flowing and rest frames. Consequently, if ω' becomes negative, the waves in our model formally adopt a negative energy density in the magnetosheath in a stationary frame. Moreover, the Poynting flux of the wave, \mathbf{S} , is given by

$$\mathbf{S} = \epsilon \mathbf{v}_g \quad (14)$$

so that the reversal in the sign of ϵ reverses the direction of \mathbf{S} (remember v_g does not change sign, see above). This obviously reverses the direction of energy propagation and can allow the magnetosheath waves to energize the magnetosphere.

Case 2 occurs when $\omega'_r = \omega_r - U k_y > 0$ and is illustrated in Figure 2a. Here $\kappa_r < 0$ and the phase of the magnetosheath waves propagates away from the boundary in both the rest (ω_r / κ_r) and the flow (ω'_r / κ_r) frames. Similarly, the waves propagate in the same direction as U downtail in both frames (i.e., ω_r / k_y and $\omega'_r / k_y > 0$). In this case the magnetopause acts as a partial reflector, $|R| < 1$, and the outgoing waves remove energy from the magnetospheric cavity, creating leaky waveguide modes which decay in time.

For sufficiently large flow speeds, ω'_r can become < 0 . This case is illustrated in Figure 2b. In this case we choose the root $\kappa_r > 0$ so that the phase and group velocity in the magnetosheath flow frame remain away from the magnetosphere (i.e., $\omega'_r / \kappa_r < 0$). In the stationary magnetosheath frame, however, the wave phase is reversed, and the wave propagates toward the magnetosphere ($\omega_r / \kappa_r > 0$). The group velocity in the stationary magnetosheath frame remains away from the magnetopause, but in this frame the waves carry negative energy. Consequently, when $\omega'_r < 0$, we have case 3 which represents overreflected waves with $|R| > 1$; the magnetosheath waves carry negative energy in a stationary frame and transport energy from the flow, across the magnetopause, and into the magnetosphere. In this overreflected case the \hat{y} phase speed in the flowing magnetosheath frame opposes U ($\omega'_r / k_y < 0$), and is opposite to the \hat{y} phase speed (ω_r / k_y) in the stationary frame. When the possibility for wave overreflection in a bounded medium is considered (for given k_y and k_z), it is clear that the upper cutoff velocity of the magnetopause instability no longer exists. This follows because for a sufficiently large flow speed, ω'_r can be-

Magnetosheath Phase Velocities

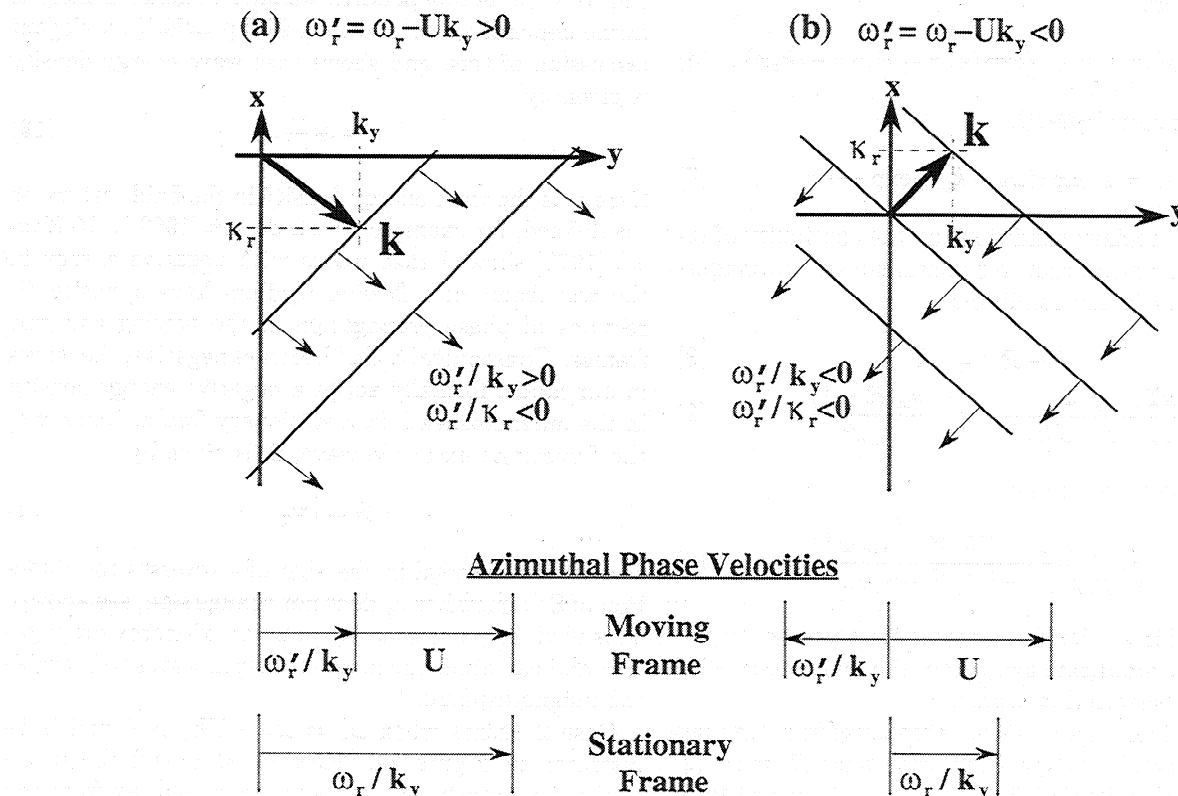


Figure 2. Schematic illustration of the waveguide mode magnetosheath phase velocities in the static (using ω_r) and the moving (using ω'_r) frames. (a) Standard (positive energy) waves which propagate away from the magnetopause in both the flowing and stationary frames. The $\hat{\mathbf{y}}$ phase velocity is in the same direction as U in both frames. (b) Overreflected (negative energy) waves which have phase propagating away from (toward) the magnetopause in the flowing (stationary) frames. In the flowing frame the waves' $\hat{\mathbf{y}}$ phase velocity propagates against the magnetosheath flow U . In the stationary frame the flow carries the waves' phase in the positive $\hat{\mathbf{y}}$ direction to create a phase speed in the positive y direction.

come < 0 , and the propagating wave solutions in the flowing medium can energize the waves trapped in the bounded medium. Rather than damping the instability by transporting energy away from the boundary, the magnetosheath waves transport energy from the background flow into the waves trapped in the magnetosphere, which grow in time. Hence, the instability can generate growing modes even for phase speeds which are superfast magnetoacoustic.

Interestingly, as pointed out by *Pu and Kivelson* [1983] (see the end of their section 3), classic KH surface waves in a compressible plasma always have real frequencies in the flow frame ω'_r which are negative (i.e., $\omega'_r = \omega_r - U k_y < 0$). Consequently, compressible KH surface waves are in fact always overreflected at the surface supporting the waves (remember that in a compressible plasma, KH surface waves have a component of phase velocity perpendicular to the boundary), even though this terminology is not normally used to describe them. Since $\omega'_r < 0$, the energy transport asso-

ciated with compressible KH wave occurs via the propagation of negative energy waves in the flowing medium.

Negative energy waves are a very interesting phenomenon, and can provide a powerful tool for estimating the instability criteria of flowing plasma configurations [e.g., *Cairns*, 1979]. Moreover, in dissipative plasmas the negative energy waves themselves can drive instabilities. If energy is lost from a negative energy wave through dissipation, its amplitude grows and it is hence unstable. Interestingly, in an unbounded tangential discontinuity between flowing incompressible dissipative media, there exists a negative energy surface wave which becomes unstable at a flow velocity slower than the lower KH cutoff velocity U_c in both hydrodynamics [e.g., *Cairns*, 1979, and references therein] and MHD [*Ruderman and Goossens*, 1995; *Joarder et al.*, 1997]. Since we are considering an ideal MHD plasma, this type of negative energy wave instability will not occur; however, it forms an interesting research area in its own right.

4. Results

4.1. Leaky Waveguide Modes

An important aspect of current waveguide mode theory is the postulate that under general magnetospheric and solar wind conditions the magnetopause can act as a near perfect reflector. We show here that the speed of the solar wind has a vital role to play in determining whether the required efficient wave trapping can take place.

Under the WKB approximation, fast magnetoacoustic modes in a box model magnetosphere [e.g., Southwood, 1974] are governed by [Inhester, 1987; Wright, 1994]

$$\frac{d^2 p_{T0}}{dx^2} + \left(\frac{\omega^2}{c_A^2(x)} - k_y^2 - k_z^2 \right) p_{T0} = 0. \quad (15)$$

where p_{T0} represents the total pressure perturbation in the magnetosphere. If, for simplicity, we assume that the magnetosheath is uniform with $c_s^2 \neq 0$ and $c_A^2 = 0$ (cf. our model in section 2), then waves there can be described by the total pressure perturbation P_{Te} and are governed by

$$\frac{d^2 p_{Te}}{dx^2} + \left(\frac{(\omega - U k_y)^2}{c_s^2} - k_y^2 - k_z^2 \right) p_{Te} = 0 \quad (16)$$

(i.e., the x wavenumbers in the magnetosphere and the magnetosheath are given by (1) and (2)). We can examine the possibility that waves may become trapped in the magnetosphere by examining the structure of the wave potentials across the magnetopause. By analogy with the one-dimensional (1-D) time independent Schrodinger equation from quantum mechanics

$$\frac{d^2 \phi}{dx^2} + \frac{2m^2}{\hbar} \{E - V(x)\} \phi = 0, \quad (17)$$

then we see that E is equivalent to $-(k_y^2 + k_z^2)$ and V is equivalent to $V_{MSP} = -\omega^2/c_A^2(x)$ in the magnetosphere and to $V_{MSH} = -(\omega - U k_y)^2/c_s^2$ in the magnetosheath, where in the quantum mechanical case ϕ is the particle's wave function, \hbar is Planck's constant $\hbar/2\pi$, m is the particle mass, E is the total energy of the particle, and $V(x)$ is the spatial form of the potential energy.

A necessary condition for wave trapping is that the wave potential increases across the magnetopause (at $x = 0$), $V_{MSP} < V_{MSH}$. For trapped wave modes with $\omega_r \neq 0$ and $\omega_i = 0$, this condition can be written as

$$\omega_r(1 - \delta) < U k_y \quad (18)$$

where $\delta = c_s/c_A$. For the magnetosphere, δ is certainly < 1 , a typical value being $\delta = 0.4$, which represents a density increase at the magnetopause $\rho_e/\rho_0 \approx 5$. Even allowing for a nonzero magnetosheath magnetic field (so that c_A in the magnetosheath is nonzero), the fast magnetoacoustic speed decreases significantly at the magnetopause so that taking $\delta < 1$ is physically reasonable.

As can be seen from (18), with $U = 0$ it is not possible to generate trapped waveguide mode solutions when $\delta < 1$. For situations where $\delta > 1$, for example, in solar coronal loops [e.g., Nakariakov and Roberts, 1995], trapped cavity modes do exist when $U = 0$ (an analysis of leaky and nonleaky waves in coronal flux tubes was addressed by Cally [1986], although the possibility for wave overreflection was not considered). In the magnetospheric case (where $\delta < 1$) these waves will be leaky in regions where U is small, such as near the subsolar point. Clearly, a consideration of variations in magnetosheath flow speed is essential in order to create modes which are trapped at particular magnetospheric local times and under particular solar wind speed conditions.

4.2. Trapped Waveguide Modes

We are interested in confining body waveguide modes inside the magnetopause. These body wave modes are spatially oscillatory in the stationary magnetospheric plasma and have phase speeds which are super-Alfvénic, that is, $\omega_r/k_y > c_A$. In our analysis a useful parameter is the phase speed normalized to the Alfvén speed in the magnetosphere, $\Omega_r = \omega_r/k_y c_A$, super-Alfvénic waves having $\Omega_r > 1$. Moreover, for trapping to occur the waves must be spatially evanescent in the flowing medium ($\kappa_r = 0, \kappa_i > 0$) so that no energy propagates across the boundary. For stable waveguide modes ($\omega_r \neq 0$ and $\omega_i = 0$), this generates the condition

$$\kappa_i^2 = k_y^2 - \frac{(\omega_r - U k_y)^2}{c_s^2} > 0 \quad (19)$$

(remember we have taken $k_z = 0$ for simplicity), which can be written as

$$U - c_s < \frac{\omega_r}{k_y} < U + c_s \quad (20)$$

(i.e., $M - \delta < \Omega_r < M + \delta$). Combining these two conditions generates a propagation band for the trapped body waveguide modes of

$$\text{Max}[c_A, U - c_s] < \frac{\omega_r}{k_y} < U + c_s \quad (21)$$

(i.e., $\text{Max}[1, M - \delta] < \Omega_r < M + \delta$). Interestingly, the condition on κ_i given in (19) can also be derived from a consideration of the wave potentials. The condition (outlined in section 4.1) that $V_{MSP} < V_{MSH}$ is a necessary but not sufficient condition for wave trapping. An additional, more restrictive, condition is that $E - V_{MSH} < 0$. This is, of course, equivalent to the condition given in (19).

In Figure 3 we show Ω_r for the body waveguide mode harmonics as a function of azimuthal wavenumber $k_y d$ for $\delta = 3$ and $M = U/c_A = 1$. Figure 3 shows that the cutoff lines (at $\Omega_r = 1$ and $\Omega_r = M + \delta$) exist as predicted by the theory [cf. Nakariakov and Roberts, 1995, Figure 1]. The upper azimuthal wavenumber ($k_y d$) cut-

Trapped Modes

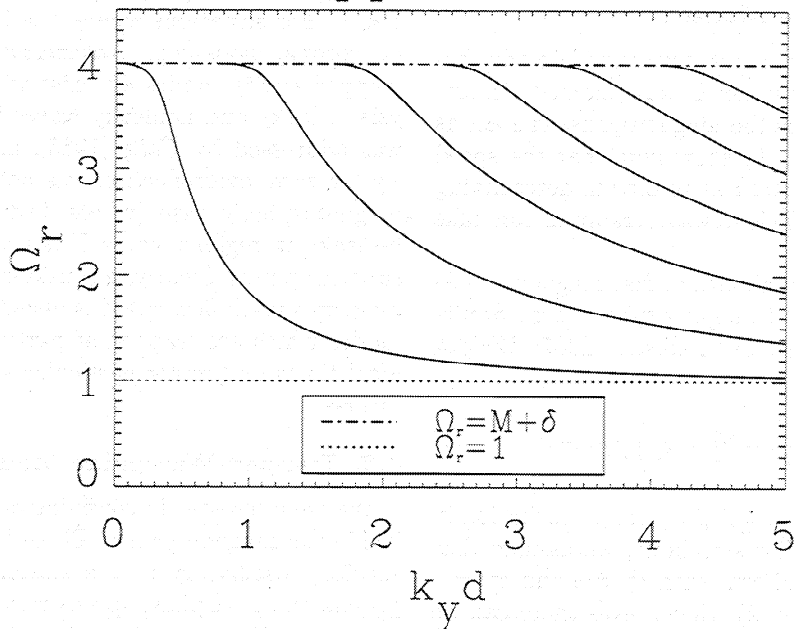


Figure 3. Trapped body waveguide mode harmonics (solid lines) for $M = 1$ and $\delta = 3$. The upper and lower wave cutoffs at $\Omega_r = M + \delta$ and $\Omega_r = \max[1, M - \delta]$ are also shown as dot-dashed and dotted lines, respectively.

off of the trapped body waveguide harmonics is defined by

$$k_y d = \frac{n\pi}{[(M + \delta)^2 - 1]^{\frac{1}{2}}} \quad n = 0, 1, 2, \dots \quad (22)$$

and occurs where $\tan k_x d = 0$, that is, $k_x d = n\pi$, in (5). For cases where $U - c_s < c_A$ (such as in Figure 3), Ω_r decreases with $k_y d$ from the upper cutoff and asymptotes to the lower cutoff at $\Omega_r = 1$, the modes remaining stable for all $k_y d$. Clearly, the first ($n = 0$) waveguide mode harmonic has no azimuthal wavenumber cutoff and exists for all $k_y d$.

In the panels in the first row of Figure 4 we show Ω_r and Ω_i (remember $\Omega_{r,i} = \omega_{r,i}/k_y c_A$) as a function of M for $\delta = 3$ (which represents a typical solar coronal loop case) and $k_y d = 2$ for the first three waveguide mode harmonics (dashed, dotted, and dot-dashed curves) and also for the unstable KH surface mode (solid curve) which exists when $U > 0$. Also shown in the left panel of this row are the (solid) lines $\Omega_r = M \pm \delta$ and $\Omega_r = M$. For $U = 0$, the first two waveguide mode harmonics are trapped ($\Omega_i = 0$), while the third (and each higher) harmonic is decaying ($\Omega_i > 0$) and represents a leaky waveguide mode having $\Omega_r > M + \delta$. As M increases, the third harmonic body waveguide mode becomes trapped once $\Omega_r < M + \delta$ at $M \approx 0.7$. (The discontinuity at this point arises from the branch cut in κ in the complex plane which results from the choice of the square root. We select the root which ensures that the phase of the waves in the flowing magnetosheath

frame remains away from the magnetopause.) The KH surface mode can be seen to asymptote to $\Omega_r, \Omega_i = 0$, and has a zero asymptotic phase speed Ω_r , as $M \rightarrow 0$. Note that in this model, the lower KH cutoff speed is zero because $\mathbf{k} \cdot \mathbf{B} = 0$ on both sides of the magnetopause. Introducing $k_z \neq 0$, or a magnetic field with a component parallel to \mathbf{k} in the magnetosheath, would introduce the usual lower KH cutoff speed; however, the qualitative results for flow speeds above the lower cutoff should remain the same. As can be clearly seen in the figure, the upper KH cutoff speed does not exist in this bounded magnetospheric model, the KH surface waves remaining unstable for any (even superfast-magnetoacoustic) flow speeds. In the second and third rows of Figure 4 we show the wavenumbers $k_x = k_{xr} + ik_{xi}$ and $\kappa = \kappa_r + i\kappa_i$. The trapped modes can be seen to have $k_{xi} = 0$ and $\kappa_r = 0$, whereas the leaky modes have $\kappa_r < 0$.

For comparison, in Figure 5 we show the behavior of the KH surface and the first three body waveguide mode harmonics as a function of M for the magnetospheric case where $\delta = 0.4$ and $k_y d = 2$. In this case, when $M = 0$, all the body waveguide mode harmonics are leaky. Similar general behavior to that in Figure 4 is observed, whereby the body modes become trapped for $\Omega_r < M + \delta$. Similarly, the KH surface mode is still unstable for all flow speeds $U > 0$ and has no upper cutoff speed. For sufficiently high flow speeds, the trapped body waveguide modes shown in Figures 4 and 5 become overreflected and grow in time, and we consider this below.

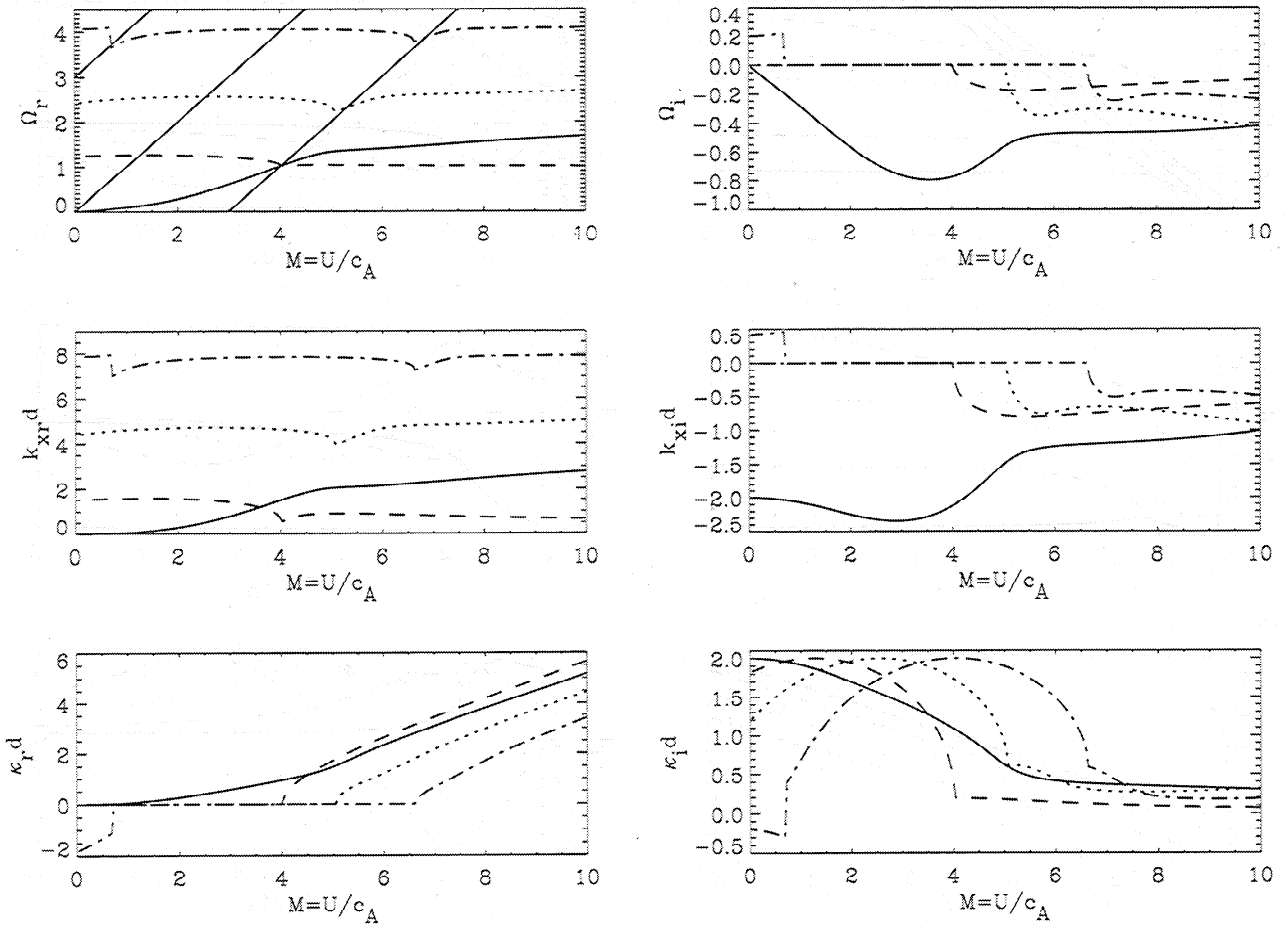


Figure 4. Ω_r and Ω_i (top row), and $k_{xr}d$, $k_{xi}d$ (middle row) and κ_{rd} and κ_{id} (bottom row), as a function of M for the first three body waveguide mode harmonics (dashed, dotted, and dot-dashed curves) and the KH surface mode (solid curve) for $\delta = 3$ and $k_yd = 2$. The top-left panel also shows the straight lines $\Omega_r = M \pm \delta$ and $\Omega_r = M$. Note that since k_yd is fixed, the normalized wave frequency $\omega_{r,i}d/c_A = \Omega_{r,i}k_yd$.

4.3. Overreflected waveguide modes

For the slow flow speed cases discussed above, where $U - c_s < c_A$ (e.g., Figure 3), overreflection never occurs and the trapped waveguide modes propagate from an upper cutoff at $\Omega_r = M + \delta$ to asymptote to $\Omega_r = 1$ as $k_yd \rightarrow \infty$. For these slow flow speeds no additional fast body modes are generated by the flows, in agreement with the conclusions of Nakariakov and Roberts [1995]. However, for sufficiently fast flow speeds, once $U - c_s > c_A$, additional stable body modes are created. Moreover, in this case at some value of k_yd , these two stable body waveguide mode branches coalesce, the resulting waves being overreflected at the magnetopause and growing in time.

The overreflected modes have $\kappa_r > 0$ (Figures 4 and 5), so that in the stationary frame the phase speed in the magnetosheath propagates toward the magnetosphere (in the flowing magnetosheath frame the waves phase speed still propagates away from the magnetosphere; see Figure 2b). These negative energy magnetosheath waves carry energy from the magnetosheath flow, across the magnetopause, into the magnetosphere

and generate growing waveguide modes whose amplification occurs by overreflection. Interestingly, and this is particularly clear in Figure 5, once the waveguide modes become unstable, the growth rate of the KH surface mode decreases drastically. Hence, in cases where body waveguide modes are energized by overreflection, the importance of the KH surface wave may be significantly reduced. Also, for very large flow speeds, Figure 5 shows that the overreflected body waveguide mode harmonics asymptotically approach constant Ω_r . In particular, this figure shows that these modes have magnetospheric wavenumbers k_x which asymptote toward $k_{xr}d = n\pi$ (and $k_{xi}d = 0$) so that the frequencies asymptote toward $\omega_r = c_A(k_{xr}^2 + k_y^2)^{1/2}$, that is, $\Omega_r = (1 + n^2\pi^2/k_y^2d^2)^{1/2}$. This means that only asymptotically, as $M \rightarrow \infty$, do the modes approach the standard (velocity) nodal magnetopause boundary condition and generate the corresponding half-wavelength modes. Under slower, more realistic, magnetosheath flow speeds, the wave modes will not form half-wavelength harmonics, and hence estimates of the eigenfrequencies of magnetospheric waveguide modes which assume a zero ve-

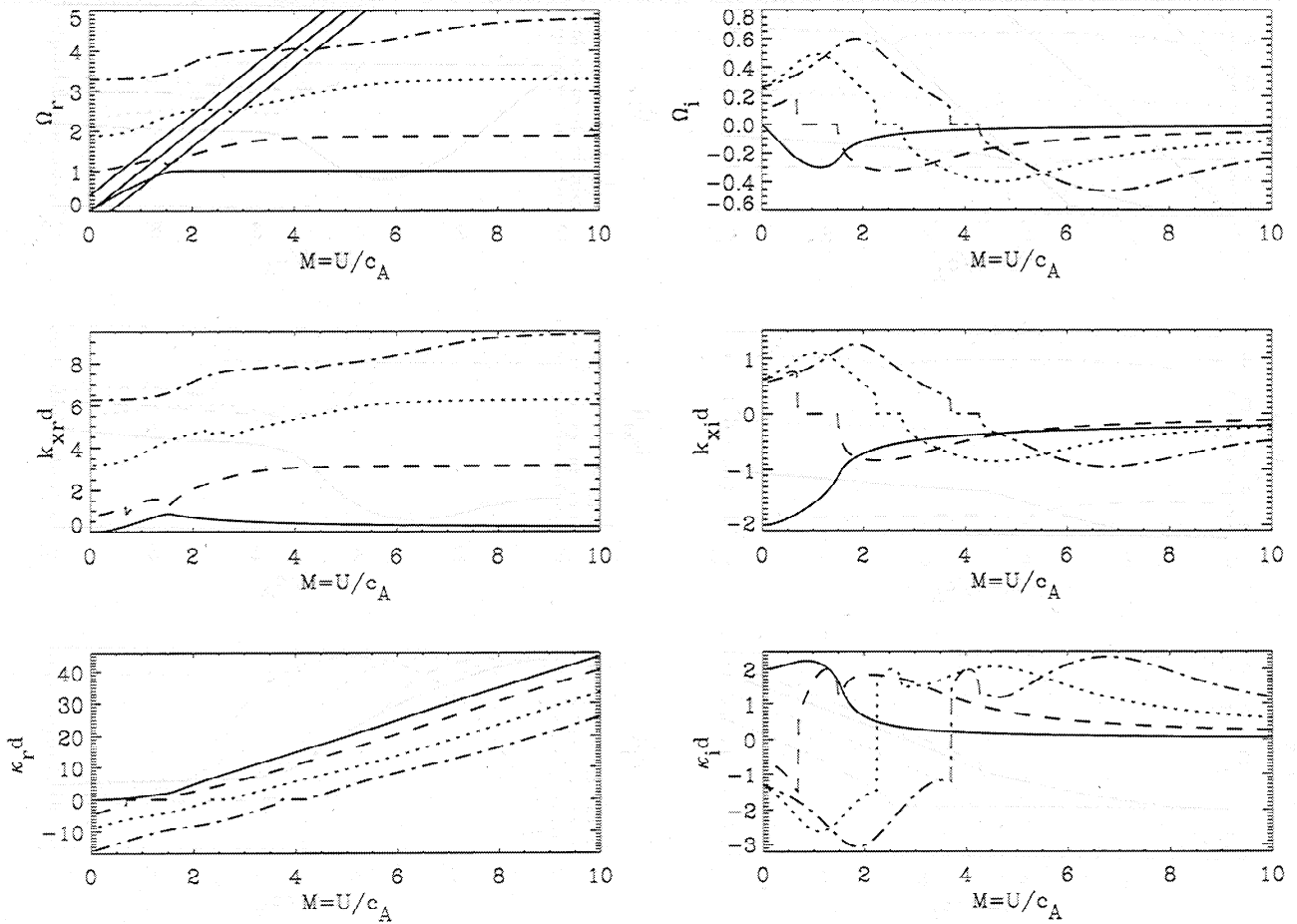


Figure 5. Ω_r and Ω_i (top row), and $k_{xr}d$, $k_{xi}d$ (middle row) and $\kappa_{r,d}$ and $\kappa_{i,d}$ (bottom row), as a function of M for the first three body waveguide mode harmonics (dashed, dotted, and dot-dashed curves) and the KH surface mode (solid curve) for $\delta = 0.4$ and $k_yd = 2$. The top-left panel also shows the straight lines $\Omega_r = M \pm \delta$ and $\Omega_r = M$. Note that since k_yd is fixed, the normalized wave frequency $\omega_{r,i}d/c_A = \Omega_{r,i}k_yd$.

velocity boundary condition at the magnetopause will be in error.

Although it might be expected that the transition to overreflection would occur at $\Omega_r = M - \delta$, in fact this only gives an approximate condition for the onset of instability. For some of the body waveguide modes, instability can occur when $\Omega_r > M - \delta$ (of course, the overreflected waves must have $\Omega_r < M$, so that $\omega' < 0$). In Figure 6 we show Ω_r for the first four body mode harmonics as a function of k_yd for $\delta = 0.4$ and $M = 2$. The upper k_yd cutoff for these modes is again given by $k_yd = n\pi/[(M + \delta)^2 - 1]^{1/2}$ (equation (22)). Now, however, since $U - c_s > c_A$, there exists another mode which propagates up from $\Omega_r = M - \delta$, being cut off at $k_yd = n\pi/[(M - \delta)^2 - 1]^{1/2}$. Physically, these additional modes represent waves which propagate in the negative y direction when $U = 0$ (i.e., against the flow when $U \neq 0$). Since the asymptote $\Omega_r = M - \delta$ represents waves which propagate against the flow at phase speed c_s in the flowing magnetosheath frame, once $U - c_s > c_A$, these modes become super-Alfvénic

in the stationary (magnetospheric) frame, can adopt a spatially oscillatory character in the magnetosphere, and hence become trapped inside the magnetopause.

At some value of k_yd , these two trapped body modes (which propagated at $\pm c_s$ in the flow frame just inside the cutoffs at $\Omega_r = M \pm \delta$) coalesce, the resulting overreflected mode becoming unstable and growing in time. Mathematically, the appearance of the additional trapped waveguide mode solutions can be demonstrated by considering the behavior of (5). For example, considering real ω and $U - c_s > c_A$, (5) possesses two real solutions for Ω_r close to $\Omega_r = M \pm \delta$ for small k_yd . As $k_yd \rightarrow \infty$, the solutions become complex, possessing nonzero ω_i , representing growing and decaying solutions, respectively (we have chosen the growing (overreflected) solution since we choose the solution with outgoing phase in the magnetosheath flow frame; see section 3). At an intermediate value of k_yd , there must be a point where there are two equal real (double) roots: this occurs at the k_yd value where (5) and $d/d\Omega_r$ of (5) are both zero. These two simultaneous equations can

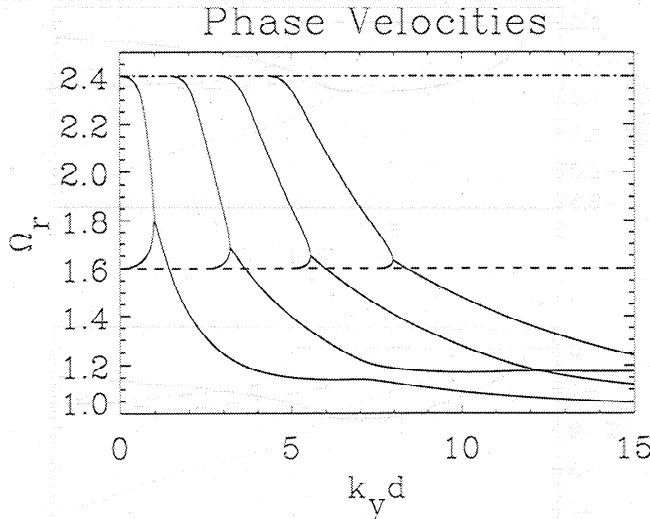


Figure 6. Ω_r as a function of $k_y d$ for the first four waveguide mode harmonics as a function of $k_y d$ for $\delta = 0.4$ and $M = 2$ (only the trapped and overreflected branches are shown for clarity).

be solved for $k_y d$ to give the $k_y d$ value for the onset of overreflection. We will not consider this in detail here; suffice it to say that numerical solution of the simultaneous equations correctly predicts the value of $k_y d$ for the onset of instability.

In Figure 7, we show the detailed behavior of the first four body waveguide mode harmonics from Figure 6 as a function of $k_y d$ (i.e., we still have $\delta = 0.4$ and $M = 2$). Again, for clarity, we have only included the stable and overreflected parts of the mode evolution and have not included the leaky waves which exist for $\Omega_r > M + \delta$. The stable ($\omega_i = 0$) modes can be seen to have $k_{xi} = 0$, $\kappa_r = 0$; the modes develop $\kappa_r > 0$ once the overreflection occurs. Interestingly, the fundamental and the third and fourth harmonics have k_{xrd} bounded as $k_y d \rightarrow \infty$, the values of k_{xrd} being given by

$$k_{xrd} = (2n + 1)\pi/2, \quad (23)$$

with $n = 1, 2, 3$. Each of these modes displays the behavior of a fastest growing mode at finite $k_y d$. The second harmonic, however, shows very similar behavior to unbounded KH surface modes, having $|\omega_i| \rightarrow \infty$ as $k_y d \rightarrow \infty$. Similarly, this second harmonic mode displays $|k_{xrd}|$, $|k_{xid}|$, $|\kappa_{rd}|$ and $|\kappa_{id}|$ all $\rightarrow \infty$. The fact that $k_{xid} \rightarrow -\infty$ and $\kappa_{id} \rightarrow \infty$ as $k_y d \rightarrow \infty$ shows that this mode exponentially decays away from the magnetopause increasingly rapidly as $k_y d \rightarrow \infty$, and hence it increasingly represents a surface type mode which is confined close to the magnetopause in this limit. This explains why the mode asymptotically behaves like a KH surface mode in an unbounded medium.

We consider this further in Figure 8, where we show the modulus of the reflection coefficient (introduced in section 3) $|R|$ as a function of $k_y d$ for the same modes as in Figure 7. Each mode, except the second harmonic,

displays a peak in $|R|$ at finite $k_y d$, the second harmonic displaying $|R| \rightarrow \infty$ as $k_y d \rightarrow \infty$. These peaks in $|R|$ match up excellently with the peaks in ω_i shown in Figure 7. Hence variations in the waves' reflection coefficient (i.e., the extent of overreflection) can explain the existence of a maximum growth rate at finite $k_y d$.

4.4. Transition From Surface to Body Modes

In a recent paper, Fujita et al. [1996] (in a similar study to ours) considered the excitation of KH surface waves in a nonuniform magnetosphere bounded from a semi-infinite flowing magnetosheath by a free sheet magnetopause. They found that for sufficiently large flow speeds ($\sim 3 - 4$ times the Alfvén speed at the magnetopause), the KH surface modes became spatially oscillatory and adopted a global character in the magnetosphere. At the same time these spatially oscillatory (body) modes displayed a maximum growth rate at finite azimuthal wavenumber, and Fujita et al. [1996] attributed this behavior to the nonuniformity of their magnetospheric Alfvén speed profile.

In Figure 9 we show the (normalized) phase velocity Ω_r of KH surface waves in our model for $\delta = 0.4$, and a range of M , as a function of $k_y d$. The KH modes have Ω_r which increases with $k_y d$ for low $k_y d$, and asymptotes to constant Ω_r at large $k_y d$. In general, the modes with asymptotic phase speeds less than c_A display the usual unbounded KH surface wave behavior with their growth rate increasing without limit as $k_y d \rightarrow \infty$. Interestingly, once the flow speed is sufficiently super-Alfvénic, this behavior changes and the waves become spatially oscillatory global modes (body waves) which exist throughout the magnetosphere. Moreover, in this case the waves display a maximum growth rate at finite $k_y d$. Since our model magnetosphere is uniform, the suggestion of Fujita et al. [1996] that a nonuniform Alfvén speed is required for this azimuthal wavenumber selection need not be satisfied. The introduction of finite depth via an inner magnetospheric boundary, and flow speeds which are sufficiently fast so the unstable modes become spatially oscillatory, are all that is required.

To illustrate the features of these two types of mode, and the transition from dominantly surface to dominantly body mode behavior, in Figure 10 we show $\omega = \omega_r + i\omega_i$, $k_x = k_{xr} + ik_{xi}$, and $\kappa = \kappa_r + i\kappa_i$ as a function of $k_y d$ for $\delta = 0.4$ at two flow speeds. The solid line represents the behavior for $M = 1$ (i.e., $|\omega_i| \rightarrow \infty$ as $k_y d \rightarrow \infty$) and relates to the left-hand side y axis scale in each panel. The dot-dashed lines represent the case $M = 2$ (i.e., $k_y d$ selection) and relate to the scales on the right-hand side of each panel (note that the transition in behavior occurs between $M = 1.6$ and $M = 1.7$). While the (low U) mode with a monotonically increasing growth rate has $|k_{xrd}|$, $|k_{xid}|$, $|\kappa_{rd}|$, and $|\kappa_{id}|$ all $\rightarrow \infty$ as $k_y d \rightarrow \infty$ (i.e., it is trapped close to the magnetopause), the mode with a maximum growth rate at

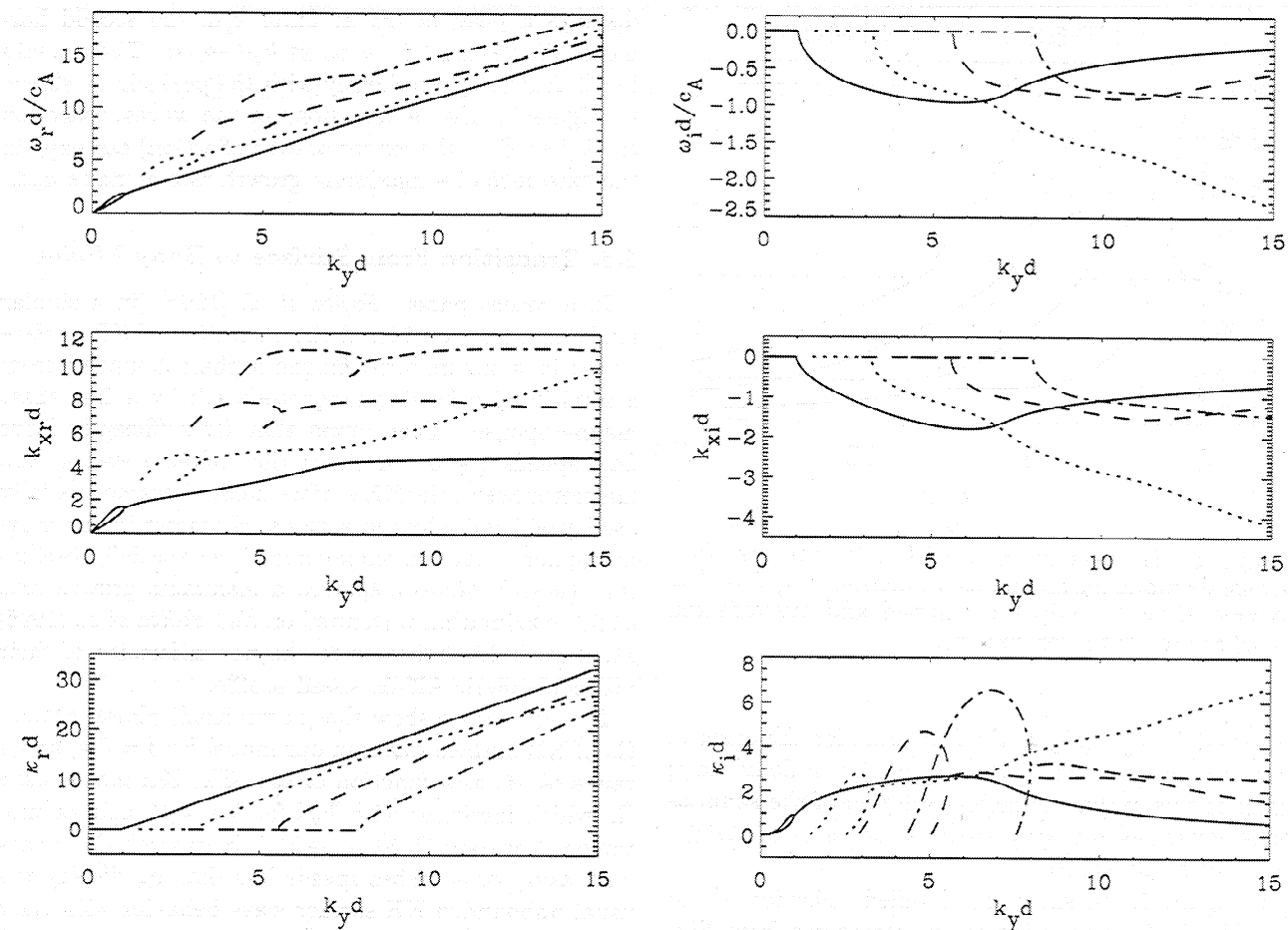


Figure 7. The first four (normalized) waveguide mode harmonic frequencies ($\omega = \omega_r + i\omega_i$), magnetospheric wavenumbers ($k_x = k_{xr} + ik_{xi}$), and magnetosheath wavenumbers ($\kappa = \kappa_r + i\kappa_i$) as a function of $k_y d$ for $\delta = 0.4$ and $M = 2$ (only the stable and overreflected branches are shown for clarity).

finite $k_y d$ displays the features that $|k_{xr}d|$ is bounded as $k_y d \rightarrow \infty$, $|k_{xi}d| \rightarrow 0$, $|\kappa_r d| \rightarrow 0$, while $|\kappa_i d|$ still $\rightarrow \infty$ (i.e., it is a dominantly body type mode in the magnetosphere). The fact that the $k_y d$ selection mode has $k_{xrd} \rightarrow \pi/2$ means that this mode approaches an antinode at the magnetopause and is hence a quarter wavelength body type mode as $k_y d \rightarrow \infty$. Moreover, we note that at the $k_y d$ values of the fastest growing modes, k_{xrd} is even less than $\pi/2$.

In a similar manner to the overreflected body waveguide modes, we can examine the existence of the azimuthal wavenumber selection by considering the behavior of the reflection coefficient R of the $M = 2$ mode. In Figure 11 we show the modulus (left-hand y axis scale, solid line) and the phase (right-hand y axis, dot-dashed line) of R as a function of $k_y d$ for the $k_y d$ selection case in Figure 10 (i.e., $\delta = 0.4$ and $M = 2$). This figure shows that $|R| = 1$ at $k_y d = 0$, and increases to a reasonably broad maximum at $k_y d \approx 2.5$, before decaying as $k_y d \rightarrow \infty$. The position of the peak in $|R|$ matches up excellently with the position of the peak in ω_i shown in Figure 10. Across the peak in $|R|$, the

phase of R changes by π . This suggests that the peak in ω_i represents the resonance of the magnetosphere in response to the magnetosheath flow.

4.5. Description of Azimuthal Wavenumber Selection

Of interest is the question of what determines whether an overreflected mode will display azimuthal wavenumber selection. Further inspection of the wave behavior shows that at the flow speed where the KH surface mode adopts $k_y d$ selection, the fundamental body mode no longer has a fastest growing mode at finite $k_y d$, that is, it displays the behavior of $|R| \rightarrow \infty$ as $k_y d \rightarrow \infty$. Physically, the surface mode changes into a body mode, while the fundamental body mode changes into a surface type mode as $k_y d \rightarrow \infty$. As U increases further, the fundamental mode regains $k_y d$ selection and becomes a body type mode, while the second harmonic waveguide mode changes to become a surface mode as $k_y d \rightarrow \infty$ and adopts a monotonically increasing growth rate (this is the case for $M = 2$ and $\delta = 0.4$, shown in Figures 7

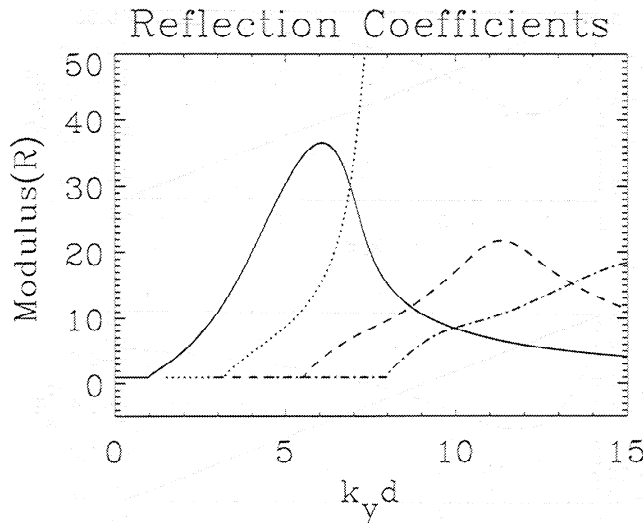


Figure 8. Modulus of the reflection coefficient R as a function of $k_y d$ for the first four waveguide mode harmonics, for $M = 2$ and $\delta = 0.4$. As in Figure 7, only the stable and overreflected branches are shown.

and 10). Increasing the flow speeds still further allows each harmonic in turn to change from a body mode, to a surface mode, and back to a body mode so that it loses and then regains a peak in ω_i at finite $k_y d$ as U increases. For any given set of overreflecting conditions, only one growing mode has the characteristic $|R| \rightarrow \infty$, the remaining modes having values of k_{xrd} which are given by the harmonic series in (23). For example, when $\delta = 0.4$ and $M = 2$ the three $k_y d$ selecting waveguide modes, along with the $k_y d$ selecting mode from Figure 10 which also exists at this flow speed, all have asymptotic k_{xrd} given by (23) with n given by $n = 0, 1, 2, 3$. While the phase change associated with the $k_y d$ selecting mode from Figure 10 simply changes by π across the peak in $|R|$ (Figure 11), the phase variation of R for the $k_y d$ selecting body modes is slightly more complicated. However, the basic feature of a peak in $|R|$ at finite $k_y d$ (the position increasing with harmonic number) is very similar. All these $k_y d$ selecting modes have dominantly body mode behavior in the magnetosphere as $k_y d \rightarrow \infty$.

Since the value of the flow speed can change the character of the modes from surface to body type, and vice versa, it is difficult to unambiguously define the characteristics of a particular mode for all values of U and $k_y d$ as they change with variations in these parameters. We originally discussed the character of the modes in terms of their behavior for small U , the modes being easily classifiable in terms of a surface or body type wave for all k_y , their characteristics as $k_y d \rightarrow \infty$ being used to determine the mode type. As discussed above, the characteristics of the modes can change as U increases, so that modes which are asymptotically (in $k_y d$) body type modes for low U can become surface modes,

and vice versa. For nonzero U the surface mode (which behaves like the unbounded KH surface mode) need not necessarily be the lowest frequency mode. However, it is only the body type modes which display azimuthal wavenumber selection. These body modes are also the only modes which will have frequencies determined by the natural frequencies of the magnetospheric cavity, and which can most easily drive monochromatic FLRs deep in the magnetosphere.

For an unbounded medium (where wavenumbers and frequencies are not constrained by the quantization imposed by the inner magnetospheric boundary) it is still possible for $|R| \rightarrow \infty$ at finite $k_y d$. Considering propagating modes, with ω , k_x , and κ all real, $|R|$ is infinite when the denominator of R is zero, that is, $k_{xrd} \rho_e (\omega_r - U k_y)^2 = \kappa_r \rho_0 \omega^2$. This represents the situation where magnetosound is spontaneously emitted from the boundary of the moving medium [e.g., Landau and Lifshitz, 1987]. Formally (in the linear case) the boundary can emit waves even in the limit that the amplitude of the incident wave tends to zero [Landau and Lifshitz, 1987]. When the form of R is written in terms of the angle of incidence θ_i , where $\theta_i = k_y/k_x = k_y c_A/\omega = \Omega^{-1}$, R can be shown to be dependent only upon θ_i , being independent of ω . For overreflected waves in a bounded medium, where ω , k_x , and κ are all complex, $|R|$ never becomes infinite at finite $k_y d$; however, the existence of the maximum in $|R|$ represents the bounded media manifestation of the unbounded spontaneous magnetosound emission. In fact, the value of θ_i which defines the maximum in R defines a fixed value of k_y/k_x . Indeed, reexamining Figures 7 and 10 shows that the first and third waveguide modes (Figure 7) and the $k_y d$ selecting mode from Figure 10 (all of which select k_y) have approximately the same

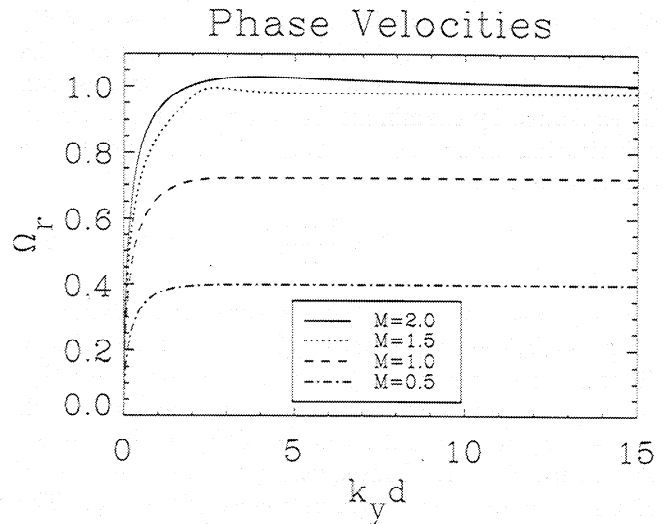


Figure 9. KH wave (normalized) y phase velocity Ω_r as a function of $k_y d$, for $\delta = 0.4$ and a range of M values.

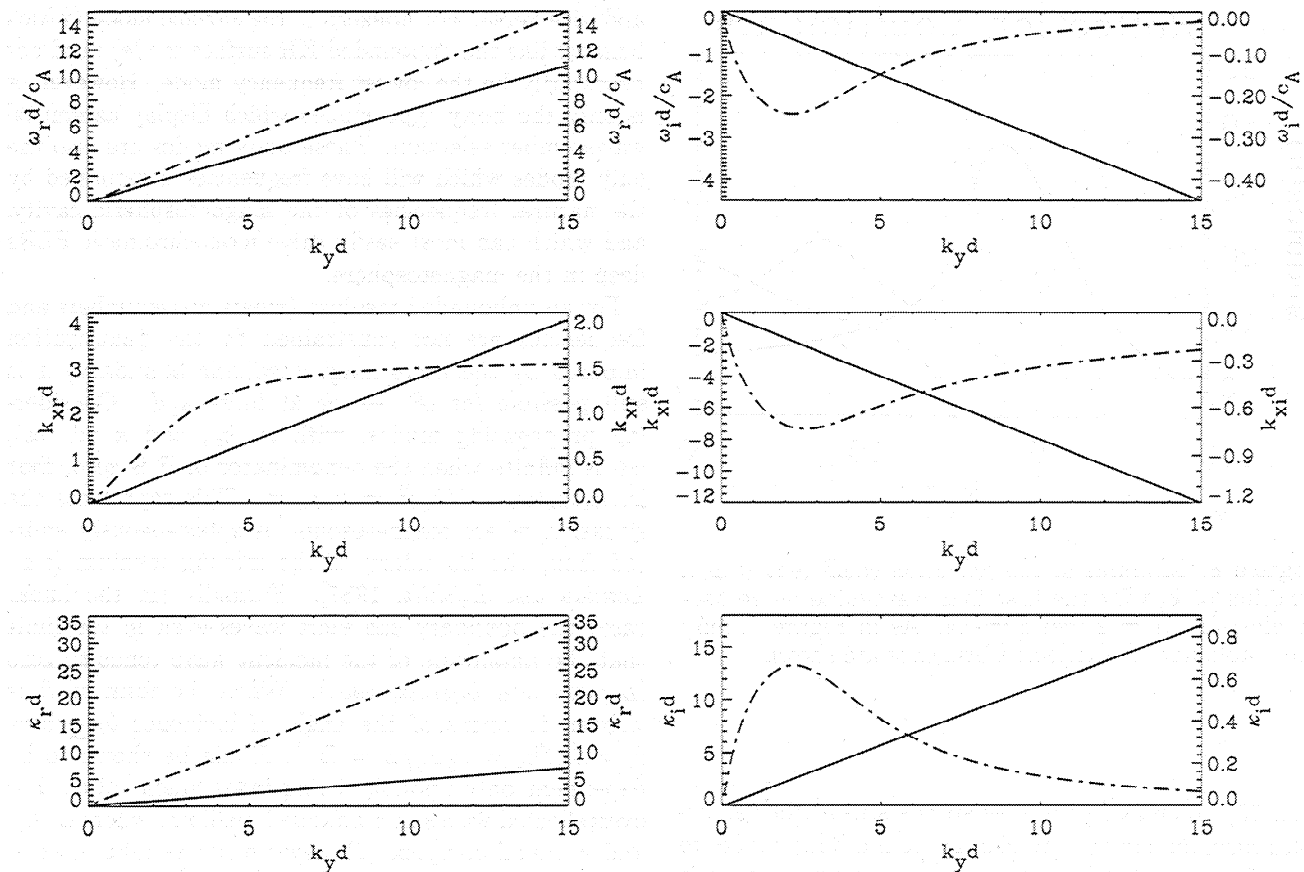


Figure 10. Normalized KH wave frequencies ($\omega = \omega_r + i\omega_i$), magnetospheric wavenumber ($k_x = k_{xr} + ik_{xi}$), and magnetosheath wavenumber ($\kappa = \kappa_r + i\kappa_i$) as a function of $k_y d$ for $\delta = 0.4$ and $M = 1$ (solid line, left-hand y axis scale) and $M = 2$ (dot-dashed line, right-hand y axis scale).

values of θ_i , that is, the phase velocities of the fastest growing body mode harmonics will all be approximately the same, as expected based on the above analysis.

Mathematically, the difference between the behavior of modes which select fastest growing waves at finite $k_y d$ (body modes amplified by overreflection) and the modes with $|\omega_i| \rightarrow \infty$ as $k_y d \rightarrow \infty$ (surface modes) can be explained by examining the complex form of R . By substituting for ω^2 and $(\omega - U k_y)^2$ from (1) and (2), we can rewrite R as

$$R = \frac{1+f}{1-f} \quad (24)$$

where $f = \kappa \rho_o c_A^2 (k_x^2 + k_y^2) / k_x \rho_e c_s^2 (\kappa^2 + k_y^2)$. Asymptotically, as $k_y d \rightarrow \infty$, at most k_x^2 and κ^2 are $\sim O(k_y^2)$. Hence, $(k_x^2 + k_y^2)/(\kappa^2 + k_y^2) \sim O(1)$, so that $f \sim \kappa/k_x$. As we have seen previously, for the surface modes with $|\omega_i| \rightarrow \infty$, both κ and k_x are $\sim O(k_y)$ as $k_y d \rightarrow \infty$, and hence $f \rightarrow 1$. Consequently, the denominator of R tends to zero, and asymptotically $|R| \rightarrow \infty$. The growing body modes, however, have bounded $k_{xr} d$, with $k_{xi}, \kappa_i \rightarrow 0$ and $\kappa_r \rightarrow \infty$ as $k_y d \rightarrow \infty$. In this case, $f \rightarrow \infty$, and $|R| \rightarrow 1$ as $k_y d \rightarrow \infty$. Between $k_y d = 0$

and $k_y d \rightarrow \infty$, $|R|$ displays a peak near the value of $k_y d$ corresponding to the fastest growing mode.

A requirement for $k_{xr} d$ to be bounded ($\sim O(1)$) as $k_y d \rightarrow \infty$ requires that $k_x^2 = k_y^2(\Omega^2 - 1)$ be $\sim O(1)$. Hence $(\Omega^2 - 1)$ must be $O(1/k_y^2)$, that is, $\Omega \sim 1 + O(1/k_y^2)$, in order for the modes to display a maximum growth rate at finite $k_y d$. Reexamining the modes in Figure 9 shows that only the $M = 2$ case (which selects $k_y d$) has $\Omega_r - 1$ decaying $\sim O(1/k_y^2)$, so that it can develop into a body mode. All the other modes shown in this figure (with $\omega_i \rightarrow \infty$ as $k_y d \rightarrow \infty$) show Ω_r increasing with $k_y d$, asymptotically toward a constant, and never decreasing $\sim O(1/k_y^2)$ as is required to keep $k_{xr} d$ bounded. Similar behavior can be seen for the waves in Figure 6. The second harmonic mode (which has $|\omega_i| \rightarrow \infty$ as $k_y d \rightarrow \infty$) displays a positive gradient $d\Omega_r/dk_y$ for large $k_y d$ and hence cannot keep $k_{xr} d \sim O(1)$, and develops into a surface mode. The first, third, and fourth harmonics, however, all have $d\Omega_r/dk_y$ negative and allow $k_{xr} d$ to remain finite as $k_y d \rightarrow \infty$, and remain body type modes.

Physically, the $k_y d$ selection which has been demonstrated above can be understood as follows. Waves

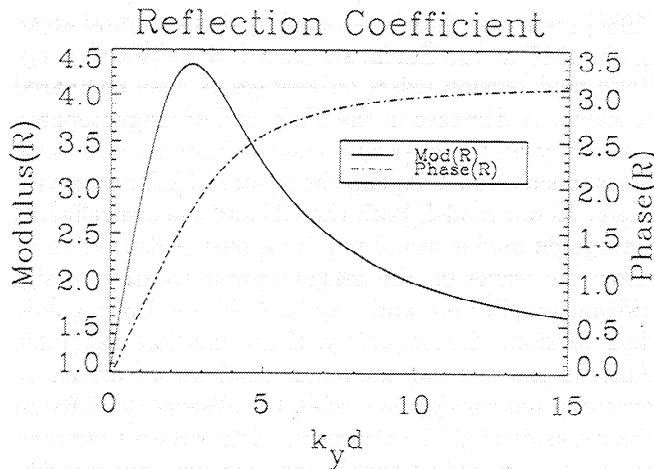


Figure 11. Modulus (solid line, left-hand y scale) and phase (dot-dashed line, right-hand scale) of the KH wave reflection coefficient R as a function of $k_y d$ for $\delta = 0.4$ and $M = 2$.

which are incident upon the magnetopause from within the magnetosphere are reflected with increased amplitude (i.e., they are overreflected). Remember that overreflected waves have a magnetosheath phase velocity which propagates toward the magnetopause in a stationary frame. Consequently, the T wave in Figure 1 adds to the amplitude $I (= 1)$ of the incident wave to generate reflected waves with $R > 1$. Since k_{xrd} is bounded for the $k_y d$ selecting body modes, at some finite value of $k_y d$ (for fixed δ and M) there is a resonance between the incident magnetosheath wave and the waves propagating with a global scale within the magnetosphere (i.e., oscillating with the natural frequency of the cavity). In contrast, the surface modes which do not select a fastest growing finite $k_y d$ have both k_x and κ which increase in a similar fashion without limit as $k_y d \rightarrow \infty$. In this case, since $|k_{xi}|$ is large, the waves remain confined close to the magnetopause and represent surface modes. For these surface waves there can be no resonance between global ringing oscillations of the magnetospheric cavity and the waves in the magnetosheath, since they are relatively unaffected by the existence of the inner magnetospheric boundary and hence display behavior similar to unbounded KH surface waves.

The behavior of the growing body modes ($k_y d$ selecting modes) is analogous to the situation which occurs if one blows (sufficiently hard) across the top of a bottle: The air in the bottle resonantly oscillates at the natural frequencies of the bottle (harmonics of the cavity inside the bottle), and the amplitude of the waves grows in response to the driver. Note that waves in the bottle would be likely to have a near antinodal boundary condition at the opening (like waves in an organ pipe). Clearly, this situation is analogous to our results

which show that the magnetopause often imposes a near antinodal boundary condition on the global scale body waves which are excited within the magnetosphere.

5. Discussion

5.1. Trapping and Excitation of Waveguide Modes

Most studies of magnetospheric waveguide modes consider the magnetopause to act as a perfect reflector [e.g., Wright, 1994]. We have shown that if the fast magnetoacoustic speed just inside the magnetopause is greater than that just outside it in the magnetosheath, which is typical, (i.e., $\delta < 1$ in our simplified model), then near the subsolar point where the magnetosheath flow speeds are small it is impossible for waveguide modes to be fully trapped inside the magnetopause. In cases where $R \lesssim 1$, then the leakage may only be small; however, when R is smaller (which is probably typical near the nose), the leakage rates will be much higher. In this case, large amounts of wave energy will be lost across the magnetopause, and hence the subsolar magnetosphere cannot act as a high-quality (Q) factor resonator for compressional $Pc5$ waves. This suggests that trapped waveguide mode theory is inapplicable to regions near the subsolar point, and that the development of well-defined resonances there may be significantly less likely than at locations where the magnetosheath flow is faster.

Under conditions of low to moderate solar wind speed, overreflection will not occur anywhere along the magnetopause, even on the flanks. In this case the subsolar magnetopause will be leaky and will hence act as a low- Q cavity. Since U increases from zero at the stagnation point at the magnetospheric nose and increases around the flanks [e.g., Spreiter and Stahara, 1980], at some point the magnetosheath flow speed should be sufficiently fast ($U > c_A - c_s$) so that the magnetopause becomes perfectly reflecting. At local times after this point, the waveguide can act as a high- Q cavity which will support narrow frequency band waveguide modes which can drive latitudinally narrow FLRs. The energy for these waveguide modes will not, however, come directly from magnetosheath flows but may be provided, for example, by solar wind impulses.

Under conditions of fast solar wind speed, waves might become overreflected on the flanks if $U > c_A + c_s$ there. Of crucial importance to our theory is the question of whether this overreflection is possible. Using the magnetic fields and densities observed just inside the magnetopause by Eastman et al. [1985] produces $c_A = 200, 500, 1500$, and 400 km s^{-1} (see their Figures 2, 3, 8, and 9 respectively and the discussion of these observations by Fujita et al. [1996]). Typically, according to the observations discussed by McKenzie

[1970] $c_s \sim 120 \text{ km s}^{-1}$, and $c_A \sim 500 \text{ km s}^{-1}$ on the flanks. Assuming that $c_A \sim 400 - 500 \text{ km s}^{-1}$ gives the condition for wave overreflection as $U \gtrsim 500 - 600 \text{ km s}^{-1}$, which could easily be satisfied for fast solar wind speeds. (Note that on the flanks the magnetosheath flow speed approaches the upstream solar wind speed [see *Spreiter and Stahara, 1980*.]) Moreover, this criterion for wave overreflection is in excellent agreement with the observations of *Kokubun et al. [1989]* and *Engelbreton et al. [1998]* that $Pc5$ azimuthal waves (FLRs) have significantly increased power when $v_{SW} > 600 \text{ km s}^{-1}$ and $v_{SW} > 500 \text{ km s}^{-1}$, respectively. In this high- v_{SW} case, the waveguide modes are energized on the flanks by magnetosheath flows. The energization occurs due to local wave overreflection at the magnetopause, and results in the transport of energy from the magnetosheath into the magnetosphere.

This variation of the likelihood of wave trapping and overreflection around the magnetopause is very interesting. $Pc5$ FLRs are most often observed on the flanks, preferentially on the dawnside; the occurrence rate for fundamental mode dawnside FLRs has a lower bound of $\sim 80\%$, that is, they are essentially continuously present there [*Anderson et al., 1990*]. Hence the observational distribution of fundamental mode $Pc5$ FLRs is in excellent agreement with the variation of both the wave trapping and overreflection conditions from the nose to the flanks of the magnetosphere. Whether the impulsive or overreflection excitation mechanisms are operative will depend upon the ambient solar wind conditions, and we discuss this further below.

A longstanding question in FLR theory is why there is such a large dawn/dusk asymmetry in FLR occurrence rates. Morning sector $Pc5$ waves are predominantly fundamental mode toroidal oscillations [e.g., *Kokubun et al., 1989; Anderson et al., 1990*]. These waves have a tendency toward oscillations with a preferred set of frequencies (around 0.8, 1.3, 1.9, 2.7, 3.3 mHz) [*Ruohoniemi et al., 1991; Samson et al., 1991; Walker et al., 1992*], which are believed to represent a discrete set of compressional waveguide mode harmonics which subsequently excite FLRs. Afternoon-side $Pc5$ waves, however, are observed to have dominantly radial and compressional components by satellites [e.g., *Kokubun et al., 1989; Anderson et al., 1990*], radars [e.g., *Chisham et al., 1995*], and ground-based magnetometers [*Rostoker and Sullivan, 1987*], with much less evidence of the waves coupling to FLRs.

One possible explanation for this involves the relative stability of KH waves on the dawn versus dusk flanks [*Lee and Olson, 1980; Miura, 1992*]. The KH instability requires a seed perturbation in order to develop to a significant amplitude. According to *Miura [1992]*, the turbulence which occurs downstream of the quasi-parallel bow shock on the dawnside may provide such a seed, whereas on the duskside, downstream of the quasi-perpendicular shock, suitable seed turbulence is likely to be much rarer. Similarly, *Lee and Olson*

[1980] point out that because of the Parker spiral angle of the IMF at the Earth, stronger KH stabilizing magnetic field tension exists on average at dusk compared to dawn. A decrease in the likelihood of magnetopause instability on the duskside, due to either or both these mechanisms, could explain the reduced FLR occurrence there. In our model, both the KH and the overreflected waveguide modes would require a seed perturbation to allow the waves on the magnetopause to grow to significant amplitudes, and may be stabilized by magnetic field tension. Consequently, if the multiple harmonic FLRs in the morningside magnetosphere are driven by overreflected waveguide modes, the absence of FLRs on the duskside could be the result of the relative rarity of the necessary seed perturbations or of excessive stabilizing magnetic tension in the afternoon magnetosheath.

Statistically, the occurrence rates of dawnside versus duskside $Pc5$ FLRs will result from a summation of waves driven either impulsively or by overreflection. Assuming that the duskside flank is relatively stable with respect to magnetopause instability and hence to overreflection, waves observed there will predominantly be impulsively excited modes, while modes on the dawnside could be excited both impulsively and by overreflection. Presumably, wave overreflection during fast solar wind conditions will provide a more efficient excitation mechanism than solar wind impulses. This would obviously explain the dawnside correlation between $Pc5$ wave power and high v_{SW} .

The observations of the afternoonside waves are consistent with the characteristics of compressional waveguide mode harmonics, and they appear to possibly display preferred discrete frequencies in accord with this hypothesis [*Chisham and Orr, 1997*]. Ground-based observations [e.g., *Ziesolleck and McDiarmid, 1994*] do show an amplitude maximum around $L \sim 7$ (where L is the McIlwain parameter), but do not display the polarization reversal characteristic of a resonance. Again, a possible explanation for this is that the afternoonside waves are driven by sudden impulses in the solar wind, rather than through wave overreflection. Significantly, the ground-based observations of afternoon $Pc5$ waves by *Rostoker and Sullivan [1987]* showed that the waves correlated with solar wind pressure variations, the magnetic signatures of the solar wind impulses being observable down to near equatorial latitudes in 75% of cases. Interestingly, these authors also observed a transition from $Pc5$ waves with no clear FLR signatures from local noon up to ~ 1600 MLT to $Pc5$ waves which displayed more classical FLR amplitude enhancements and polarization reversals after 1600 MLT. This is entirely consistent with afternoonside waves being dominantly impulsively driven, and with the existence of a transition from a low- Q to a high- Q cavity around the afternoon flank. *Olson and Rostoker [1978]* reported similar characteristics to *Rostoker and Sullivan [1987]* in their afternoonside $Pc5$ waves. Their waves displayed reduced amplitudes near noon (consistent with a leaky magne-

topause), and on the afternoonside had more complex and irregular (nonsinusoidal) signatures (both in terms of their waveform and envelope variations) than waves observed near dawn. All of these observations point to a distinction between impulsively excited afternoonside and dominantly overreflected dawnside $Pc5$ waves, and suggest that the subsolar magnetopause acts locally as a low- Q leaky waveguide.

Since it is unlikely that the subsolar magnetopause can act as a high- Q cavity, waves which are impulsively driven near the subsolar point in this (leaky) waveguide will necessarily have a broad frequency bandwidth and will be unlikely to able to excite a narrow FLR response. Interestingly, recent observations using multiple satellites and ground-based magnetometers have demonstrated the downtail propagation of an impulsively driven compressional waveguide mode for the first time [Mann et al., 1998]. Indeed, the ground-based magnetometers in this study (near local noon) did not show any FLR characteristics, although as stated by these authors, FLRs might have been driven at local times displaced from their observations. In fact, Mann et al. [1998] observed a decrease in waveguide mode power of $\sim 38\%$ between their observation with Active Magnetospheric Particle Tracer Explorers (AMPTE) CCE near local noon and AMPTE UKS/IRM $6.2R_E$ away on the morning flank. Assuming that the waveguide mode did not drive any strong FLRs between these two observations, this is consistent with waveguide mode energy leaking out of the cavity (note, however, that energy can also leak out of the polar cap as well as out through a leaky magnetopause boundary). The combination of both the magnetopause stability and the low Q of impulsively driven waveguide modes could explain the lack of any significant FLR signatures in the afternoon. Of course, we expect field line resonance signatures near the dawn flank to be dominated by overreflected waves. At times when overreflection is operative, these field lines could be nearly continually driven. This would, of course, allow dawnside $Pc5$ waves to develop FLR characteristics at the same frequencies as the compressional waveguide mode harmonics.

5.2. Azimuthal Wavenumber Selection

Observations of FLRs, believed to be driven by compressional waveguide modes harmonics, generally show the dominance of a particular azimuthal wavenumber (m , equivalent to $k_y d$); m tends to increase with wave frequency and hence, by implication, with waveguide harmonic. Ziesolleck and McDiarmid [1994] analyzed the azimuthal phase speed of multiple dawnside FLRs on different days. They found that in general ω_r/k_y was the same for all the FLR harmonics observed simultaneously (i.e., the phase velocity was independent of frequency; see also Olson and Rostoker [1978]); however, this (constant) phase speed varied from day to day.

In general, cavity mode theories consider m to be a free parameter. Our model shows how the coupling of the magnetosheath to the magnetosphere via a free magnetopause boundary can generate m selection, in accord with the m selection for global KH modes demonstrated by Fujita et al. [1996]. As is clearly shown by our results, the dominant azimuthal wavenumber increases with waveguide mode frequencies, so that our model is consistent with the observed dependence of m on frequency.

Waveguide models (with a perfectly reflecting magnetopause) allow the excitation of modes with a range of m values, theory predicting that the lowest m modes will have the lowest downtail group speed and hence be most likely to act as long-lived and coherent drivers for FLRs in the near Earth waveguide [e.g., Wright, 1994; Rickard and Wright, 1994]. Wright and Rickard [1995b], using their perfectly reflecting magnetopause waveguide model, found that stimulating a tailward running pulse on the magnetopause drove FLR harmonics whose phase velocities were constant for a given magnetopause wave propagation speed, whereas FLRs driven by impulses near the nose excited waveguide modes with different phase velocities for different harmonics. This provides a possible diagnostic to distinguish between impulsively and overreflection driven waves. As we discussed in section 4, the phase velocities of the fastest growing components of the overreflected waveguide mode harmonics all have approximately the same phase velocity, and will be similar to the running pulse driver considered by Wright and Rickard [1995a]. Consequently, we suggest that the waves observed by Ziesolleck and McDiarmid [1994] are in fact driven by overreflected waveguide modes. If this is the case, the phase velocities should be correlated with U , larger U generating larger azimuthal phase velocities. It would be interesting to know whether such a correlation exists experimentally, and whether the largest FLR phase velocities observed by Ziesolleck and McDiarmid [1994] were observed during the times of fastest solar wind speed.

Our model also predicts that the lowest waveguide mode harmonics will be the easiest to excite, since they become trapped or overreflected at lower solar wind speeds. Ground-based magnetometer studies at both high [Ziesolleck and McDiarmid, 1995] and low [Ziesolleck and Chamalaun, 1993] latitudes have found a tendency for higher frequency FLRs to be driven with enhanced power during more active magnetospheric conditions (they considered correlations with K_p). This is also in accord with our model, since higher magnetosheath speeds allow higher waveguide mode harmonics to lose their leaky behavior and become trapped or energized by overreflection on the flanks. Hence these higher harmonic waveguide modes will be more likely to be able to drive FLRs in the magnetosphere during more active (presumably higher solar wind speed) conditions (note that although magnetic activity corre-

lates with the southward component of the IMF, it also has a dependence on solar wind speed). The particular FLR harmonic which displays dominant power in the magnetosphere will depend not only on solar wind speed (which will determine which modes can become overreflected and what their relative growth rates will be), but also upon the relative coupling strengths of the waveguide modes to Alfvén resonances which are a function of their m value [e.g., *Kivelson and Southwood*, 1986].

Implicit in our model, because we have used an infinitesimal magnetopause, is the assumption that wave scale lengths are much larger than the width of the velocity shear (i.e., the width of the low latitude boundary layer (LLBL)). Once the finite thickness of the velocity shear is included, the higher k_y modes become stabilized [*Ong and Roderick*, 1972; *Walker*, 1981]. Indeed, *Walker* [1981] found that the peak KHI growth rate occurred when $k\Delta \sim 0.6$, where Δ is the half width of the velocity shear layer, which is $\sim 0.5R_E$ on the flanks [*Yumoto and Saito*, 1980]. Considering a magnetospheric depth of $\sim 15R_E$ on the flanks (i.e., $d = 15R_E$), then the peak in $k_y d$ which would occur in our model due to a finite LLBL width would occur at $k_y d \sim 18$. Consequently, our results for wave growth rates will decrease above $k_y d \sim 18$ due to the existence of the finite width of the LLBL. Clearly, however, the feature of $k_y d$ value selection for the low waveguide mode harmonics will remain, the values of the dimensionless azimuthal wavenumbers $k_y d$ being in good agreement with the range of observed flank FLR m values, typically $m \lesssim 10$.

Since the KH surface mode can have a growth rate which is larger than the overreflected body modes (especially at lower flow speeds), it is important to consider why $k_y d \sim 18$ KH waves do not dominate the waves observed in the magnetosphere (remember, however, that once the magnetosheath flow is sufficient for the body waveguide modes to grow via overreflection, the growth rate of the KH surface modes drastically reduced; see Figures 4 and 5). One reason may be that the large m (or $k_y d$) KH surface waves are confined to a velocity boundary layer (VBL) region close to the magnetopause. These disturbances may be swept downstream, or they may saturate nonlinearly, producing a turbulent boundary layer of finite thickness. The penetration distance for KH surface waves into the magnetosphere is given by $l_{x,sp} = 1/[k_y(1 - \Omega_r^2)^{\frac{1}{2}}]$ [*Miura*, 1992, equation (19)]; this result is verified by Miura's simulations which show that the majority of the KH surface waves' energy density is confined in a VBL of this width [see *Miura*, 1992]. Typically for KH surface modes, $\Omega_r \sim 0.7 - 0.8$ for the fastest growing mode (taking $M \sim 1.0 - 1.3$ from Figure 9) so that $l_{x,sp} \sim 1.4 - 1.7k_y^{-1} = 1.2 - 1.4R_E$. Indeed, the VBL in Miura's simulations typically has a full width of $\sim 3\Delta$ (i.e., $\sim 1.5R_E$ on the flanks) (see, for example, Figure 6 of *Miura* [1990]), in good agreement with the scale size of the fastest growing linear KH surface mode discussed

above. Since the thickness of the VBL is small compared to the wavelength of the lowest harmonic waveguide modes, the shear layer may be approximated as a discontinuity, and the analysis in this paper should be applicable.

5.3. Waveguide Mode Eigenfrequencies

An outstanding problem in magnetospheric waveguide theory is why the eigenfrequencies of the magnetospheric cavity are so low (i.e., a few millihertz). The theoretical waveguide eigenfrequencies can be calculated by considering the natural frequencies of the 2-D (radial and field aligned) cavities which make up cross sections of the waveguide. In fact, allowing the waveguide modes to have finite (low) values of k_y has little effect on the natural frequencies of the waveguide modes, since for fast waves in a dipole geometry $L_y \gg L_x$ and L_z . Hence k_y variation only introduces a small additional frequency bandwidth into the waveguide modes [e.g., *Lee*, 1996].

A simplified 1-D WKB model [*Samson et al.*, 1991, 1992] was able to generate discrete waveguide mode frequencies in accordance with the discrete FLR frequencies observed with HF radar discussed above, with the exception of the lowest (0.8 mHz) frequency. As discussed by *Walker et al.* [1992], it is very difficult to reconcile this lowest frequency with the eigenfrequency of a perfectly reflecting cavity of sensible dimensions and realistic plasma density. However, the calculations of *Samson et al.* [1991, 1992] required a rather large central plasma sheet density of $\gtrsim 25 \text{ m}_p/\text{cm}^3$ to obtain eigenfrequencies which matched a harmonic series of FLRs with a fundamental mode frequency of 1.3 mHz (see the discussion of *Harrold and Samson* [1992]). Moreover the 1-D model of *Samson et al.* [1991, 1992] generates field lines which have lengths which decrease with increasing L shell, so that this model is not a good approximation to reality [*Allan and McDiarmid*, 1993].

Using more realistic 2-D cavity models, such as a dipole, will produce higher waveguide eigenfrequencies by including the field-aligned variation of the compressional waveguide modes more self-consistently [*Lee*, 1996]. Combining this with more realistic plasma densities will increase the frequencies of the eigenmodes even further. To try to circumvent some of these problems, *Harrold and Samson* [1992] proposed an extension of the trapping cavity out to the bow shock rather than just to the magnetopause. In their model, the reflectivity of the magnetopause was low, and because of both the extension of the dimensions of the cavity and the low sound and Alfvén speeds in the magnetosheath it was able to significantly lower the eigenfrequencies of the waveguide modes. All these studies assume that the outer boundary (usually the magnetopause, but also the bow shock) acts as a perfect reflector, so that the waveguide modes possess a nodal boundary condition there.

In contrast, our results show that the overreflected cavity modes, which we propose are the drivers of the observed discrete FLRs, more closely adopt an antinodal boundary condition at the magnetopause, the radial (x) wavenumbers k_{xr} (equation (23)) in our uniform magnetospheric model forming a harmonic series of near quarter-wavelength modes. Allowing the magnetopause to impose a near antinodal boundary condition can significantly lower the eigenfrequencies of the overreflected modes which are supported by the waveguide bounded by the magnetopause. Models which incorporate this boundary condition in a realistic simulation may be able to produce approximately millihertz eigenfrequencies between the magnetopause and an inner wave turning point without having to resort to the adoption of unusually high values for magnetospheric plasma density.

6. Conclusions

We have presented a model for the excitation of magnetospheric waveguide modes by considering a bounded magnetosphere coupled to a semi-infinite flowing magnetosheath by a sheet magnetopause. This model can explain a number of features of $Pc5$ FLRs, which are believed to be driven by the compressional modes supported by the waveguide:

1. Body type waveguide modes, with phase speeds greater than the fast magnetoacoustic speed, have frequencies which are determined by the natural frequencies of the waveguide. In contrast to models which previously assumed that these modes could be trapped inside a perfectly reflecting magnetopause, we find that near the subsolar point they are usually leaky, wave trapping only being possible further toward the flanks where the magnetosheath flow speed is sufficiently fast so that $U + c_s > c_A$, where c_s is the sound speed in the magnetosheath, and c_A is the Alfvén speed just inside the magnetopause and U is the magnetosheath flow speed.

2. For conditions of fast solar wind speed, so that the condition $U > c_s + c_A$ can be satisfied on the flanks, flank waveguide modes can become overreflected, grow in time, and be energized by the transport of energy across the magnetopause into the magnetosphere.

3. Both the wave trapping and overreflection conditions are more easily satisfied on the flanks of the magnetosphere, at the locations where $Pc5$ FLRs are most often observed.

4. Observations show a correlation between increased $Pc5$ wave power and solar wind speeds which exceed $\sim 500\text{-}600 \text{ km s}^{-1}$. This threshold for significant $Pc5$ wave power fits excellently with the criterion that energization via overreflection is only possible once $U > c_s + c_A$.

5. Overreflected waveguide modes display azimuthal wavenumber selection, higher harmonics having higher dominant azimuthal wavenumbers in accordance with observations.

6. The overreflected waves are subject to a near antinodal boundary condition at the magnetopause, and represent quarter-wavelength radial harmonics.

7. Adopting this antinodal magnetopause boundary condition, rather than the usually assumed nodal condition, can considerably lower the eigenfrequencies in a given model waveguide. Hence this modified boundary condition may be able to explain the generation of millihertz frequency waveguide mode harmonics in a realistic model without resorting to unreasonably high magnetospheric plasma densities.

8. Understanding the local time distributions of the locations of wave trapping and overreflection can help to distinguish between different possible $Pc5$ FLR wave sources, and may provide an explanation for the long observed dawn/dusk asymmetry in the occurrence of FLRs. Future studies should examine realistic variations of the Alfvén, sound, and flow speeds around the magnetopause and determine at which locations it is possible for waves to be either trapped or overreflected. Near the subsolar point the magnetopause is leaky, so that the magnetosphere is unable to act as a high- Q resonant cavity for compressional $Pc5$ waveguide modes there. Moreover, since U is low near the nose, it is very unlikely that overreflected waveguide modes will be excited there. As we discussed above, however, on the flanks where the magnetosheath flow speed is increased, waves are much more likely to be trapped and can be overreflected under conditions of fast solar wind speed. The general observational distributions of $Pc5$ wave power mirror the local time distributions of the likely regions of waveguide mode overreflection, especially if the duskside magnetopause is stable with respect to overreflection, so that the waveguide modes needed to drive FLRs cannot grow there.

Acknowledgments. ANW was supported by a PPARC Advanced Fellowship, VMN was supported by a PPARC postdoc, and KM was supported by a PPARC Research Studentship. The authors thank A. D. M. Walker for providing a prepublication copy of his 1998 paper which inspired the production of Figures 8 and 11, and thank M. Ruderman for helpful comments on the manuscript.

The Editor thanks William Allan and another referee for their assistance in evaluating this paper.

References

- Allan, W., and D. R. McDiarmid, Frequency ratios and resonance positions for magnetospheric cavity/waveguide modes, *Ann. Geophys.*, **11**, 916, 1993.
- Allan, W., S. P. White, and E. M. Poulter, Magnetospheric coupling of hydromagnetic waves - Initial results, *Geophys. Res. Lett.*, **12**, 287, 1985.
- Allan, W., S. P. White, and E. M. Poulter, Impulse-excited hydromagnetic cavity and field-line resonances in the magnetosphere, *Planet. Space Sci.*, **34**, 371, 1986.
- Anderson, B. J., M. J. Engebretson, S. P. Rounds, L. J. Zanetti, and T. A. Potemra, A statistical study of pulsations observed by the AMPTE/CCE magnetic fields experiment, I, Occurrence distributions, *J. Geophys. Res.*, **95**, 10,495, 1990.

- Anderson, J. E., *Magnetohydrodynamic Shock Waves*. M.I.T. Press, Cambridge, Mass., 1963.
- Cairns, R. A., The role of negative energy waves in some instabilities of parallel flows, *J. Fluid Mech.*, 92, 1, 1979.
- Cally, P. S., Leaky and non-leaky oscillations in magnetic flux tubes, *Solar Phys.*, 103, 277, 1986.
- Chandrasekhar, S., *Hydrodynamic and Hydromagnetic Stability*. Oxford Univ. Press, New York, 1961.
- Chen, L., and A. Hasegawa, A theory of long-period magnetic pulsations, 1, Steady state excitation of field line resonance, *J. Geophys. Res.*, 79, 1024, 1974a.
- Chen, L., and A. Hasegawa, A theory of long-period magnetic pulsations, 2, Impulsive excitation of surface eigenmode, *J. Geophys. Res.*, 79, 1033, 1974b.
- Chisham, G., and D. Orr, A statistical study of the local time asymmetry of Pc5 ULF wave characteristics observed at mid-latitudes by SAMNET, *J. Geophys. Res.*, 102, 24,339, 1997.
- Chisham, G., D. Orr, T. K. Yeoman, D. K. Milling, M. Lester, and J. A. Davies, The polarisation of Pc5 ULF waves around dawn: A possible ionospheric conductivity gradient effect, *Ann. Geophys.*, 13, 159, 1995.
- Dungey, J. W., Electrodynamics of the outer atmosphere, in *Proceedings of the Ionosphere*, p. 255. Phys. Soc. of London, London, 1955.
- Eastman, T. E., B. Popielawska, and L. A. Frank, Three-dimensional plasma observations near the outer magnetospheric boundary, *J. Geophys. Res.*, 90, 9519, 1985.
- Engebretson, M., K.-H. Glassmeier, M. Stellmacher, W. J. Hughes, and H. Luhr, The dependence of high latitude Pc5 wave power on solar wind velocity and on the phase of high speed solar wind streams, *J. Geophys. Res.*, in press, 1998.
- Fejer, J. A., Hydromagnetic stability at a fluid discontinuity between compressible fluids, *Phys. Fluids*, 7, 499, 1964.
- Fujita, S., K.-H. Glassmeier, and K. Kamide, MHD waves generated by the Kelvin-Helmholtz instability in a nonuniform magnetosphere, *J. Geophys. Res.*, 101, 27,317, 1996.
- Harrold, B. G., and J. C. Samson, Standing ULF modes of the magnetosphere: A theory, *Geophys. Res. Lett.*, 19, 1811, 1992.
- Inhester, B., Numerical modeling of hydromagnetic wave coupling in the magnetosphere, *J. Geophys. Res.*, 92, 4751, 1987.
- Joarder, P. S., V. M. Nakariakov, and B. Roberts, A manifestation of negative energy waves in the solar atmosphere, *Solar Phys.*, 176, 285, 1997.
- Kivelson, M. G., and D. J. Southwood, Resonant ULF waves: A new interpretation, *Geophys. Res. Lett.*, 12, 49, 1985.
- Kivelson, M. G., and D. J. Southwood, Coupling of global magnetospheric MHD eigenmodes to field line resonances, *J. Geophys. Res.*, 91, 4345, 1986.
- Kivelson, M. G., J. Etcheto, and J. G. Trotignon, Global compressional oscillations of the terrestrial magnetosphere: The evidence and a model, *J. Geophys. Res.*, 89, 9851, 1984.
- Kokubun, S., K. N. Erickson, T. A. Fritz, and R. L. McPherron, Local time asymmetry of Pc4-5 pulsations and associated particle modulations at synchronous orbit, *J. Geophys. Res.*, 94, 6607, 1989.
- Lamb, H., *Hydrodynamics*. Dover, New York, 1932.
- Landau, L. D., and E. M. Lifshitz, *Fluid Mechanics*. Pergamon, Oxford, 1987.
- Lee, D.-H., Dynamics of MHD wave propagation in the low-latitude magnetosphere, *J. Geophys. Res.*, 101, 15,371, 1996.
- Lee, L. C., and J. V. Olson, Kelvin-Helmholtz instability and the variation of geomagnetic pulsation activity, *Geophys. Res. Lett.*, 7, 777, 1980.
- Lerche, I., Validity of the hydromagnetic approach in discussing instability of the magnetospheric boundary, *J. Geophys. Res.*, 71, 2365, 1966.
- Mann, I. R., G. Chisham, and S. D. Bale, Multisatellite and ground-based observations of a tailward propagating Pc5 magnetospheric waveguide mode, *J. Geophys. Res.*, 103, 4657, 1998.
- McKenzie, J. F., Hydromagnetic wave interaction with the magnetopause and the bow shock, *Planet. Space Sci.*, 18, 1, 1970.
- Miura, A., Kelvin-Helmholtz instability for supersonic shear flow at the magnetospheric boundary, *Geophys. Res. Lett.*, 17, 749, 1990.
- Miura, A., Kelvin-Helmholtz instability at the magnetopause boundary: Dependence on the magnetosheath sonic Mach number, *J. Geophys. Res.*, 97, 10,655, 1992.
- Miura, A., and P. L. Pritchett, Nonlocal stability analysis of the MHD Kelvin-Helmholtz instability in a compressible plasma, *J. Geophys. Res.*, 87, 7431, 1982.
- Nakariakov, V. M., and B. Roberts, Magnetosonic waves in structured atmospheres with steady flows, 1, Magnetic slabs, *Solar Phys.*, 159, 213, 1995.
- Olson, J. W., and G. Rostoker, Longitudinal phase variations of Pc4-5 micropulsations, *J. Geophys. Res.*, 83, 2481, 1978.
- Ong, R. S. B., and N. Roderick, On the Kelvin-Helmholtz instability of the Earth's magnetopause, *Planet. Space Sci.*, 20, 1, 1972.
- Papamoshov, D., and A. Roshko, The compressible turbulent shear layer: An experimental study, *J. Fluid Mech.*, 197, 453, 1988.
- Parker, E. N., Dynamics of the interplanetary gas and magnetic fields, *Astrophys. J.*, 128, 664, 1958.
- Pu, Z. Y., and M. G. Kivelson, Kelvin-Helmholtz instability at the magnetopause: Solution for compressible plasmas, *J. Geophys. Res.*, 88, 841, 1983.
- Rickard, G. J., and A. N. Wright, Alfvén resonance excitation and fast wave propagation in magnetospheric waveguides, *J. Geophys. Res.*, 99, 13,455, 1994.
- Roberts, B., MHD waves in the sun, in *Advances in Solar System Magnetohydrodynamics*, edited by E. R. Priest, and A. W. Hood, p. 105. Cambridge Univ. Press, New York, 1991.
- Rostoker, G., and B. T. Sullivan, Polarisation characteristics of Pc5 magnetic pulsations in the dusk hemisphere, *Planet. Space Sci.*, 35, 429, 1987.
- Ruderman, M. S., and M. Goossens, Surface Alfvén waves of negative energy, *J. Plasma Phys.*, 54, 149, 1995.
- Ruohoniemi, J. M., R. A. Greenwald, K. B. Baker, and J. C. Samson, HF radar observations of field line resonances in the midnight/early morning sector, *J. Geophys. Res.*, 96, 15,697, 1991.
- Samson, J. C., R. A. Greenwald, J. M. Ruohoniemi, T. J. Hughes, and D. D. Wallis, Magnetometer and radar observations of magnetohydrodynamic cavity modes in the Earth's magnetosphere, *Can. J. Phys.*, 69, 929, 1991.
- Samson, J. C., B. G. Harrold, J. M. Ruohoniemi, and A. D. M. Walker, Field line resonances associated with MHD waveguides in the magnetosphere, *Geophys. Res. Lett.*, 19, 441, 1992.
- Sen, A. K., Effect of compressibility on Kelvin-Helmholtz instability in a plasma, *Phys. Fluids*, 7, 1293, 1964.
- Southwood, D. J., The hydromagnetic stability of the magnetospheric boundary, *Planet. Space Sci.*, 16, 587, 1968.
- Southwood, D. J., Some features of field line resonances in the magnetosphere, *Planet. Space Sci.*, 22, 483, 1974.

- Southwood, D. J., and M. G. Kivelson, The magnetohydrodynamic response of the magnetospheric cavity to changes in solar wind pressure, *J. Geophys. Res.*, **95**, 2301, 1990.
- Spreiter, J. R., and S. S. Stahara, A new predictive model for determining solar wind-terrestrial planet interactions, *J. Geophys. Res.*, **85**, 6769, 1980.
- Walker, A. D. M., The Kelvin-Helmholtz instability in the low-latitude boundary layer, *Planet. Space Sci.*, **29**, 1119, 1981.
- Walker, A. D. M., J. M. Ruohoniemi, K. B. Baker, and R. A. Greenwald, Spatial and temporal behavior of ULF pulsations observed by the Goose Bay HF radar, *J. Geophys. Res.*, **97**, 12,187, 1992.
- Wright, A. N., Dispersion and wave coupling in inhomogeneous MHD waveguides, *J. Geophys. Res.*, **99**, 159, 1994.
- Wright, A. N., and G. J. Rickard, A numerical study of resonant absorption in a magnetohydrodynamic cavity driven by a broadband spectrum, *Astrophys. J.*, **444**, 458, 1995a.
- Wright, A. N., and G. J. Rickard, ULF pulsations driven by magnetopause motions: Azimuthal phase characteristics, *J. Geophys. Res.*, **100**, 23,703, 1995b.
- Yumoto, K., and T. Saito, Hydromagnetic waves driven by velocity shear instability in the magnetospheric boundary layer, *Planet. Space Sci.*, **28**, 789, 1980.
- Ziesolleck, C. W. S., and F. H. Chamalaun, A two-dimensional array study of low-latitude Pc5 geomagnetic pulsations, *J. Geophys. Res.*, **98**, 13,703, 1993.
- Ziesolleck, C. W. S., and D. R. McDiarmid, Auroral latitude Pc5 field line resonances: Quantized frequencies, spatial characteristics, and diurnal variation, *J. Geophys. Res.*, **99**, 5817, 1994.
- Ziesolleck, C. W. S., and D. R. McDiarmid, Statistical survey of auroral latitude Pc5 spectral and polarization characteristics, *J. Geophys. Res.*, **100**, 19,299, 1995.

I. R. Mann, Department of Physics, University of Alberta, Edmonton, Alberta, Canada, T6G 2J1. (e-mail: ian@aurora.york.ac.uk)

K. J. Mills, V. M. Nakariakov, and A. N. Wright, Mathematical Institute, University of St. Andrews, St. Andrews, Fife, Scotland, KY16 9SS. (e-mail: katie@dcs.st-and.ac.uk; valery@dcs.st-and.ac.uk; andy@dcs.st-and.ac.uk)

(Received April 1, 1998; revised August 13, 1998; accepted September 10, 1998.)